JBC RESEARCH ARTICLE

Unusual reactivity of a flavin in a bifurcating electron-transferring flavoprotein leads to flavin modification and a charge-transfer complex

Received for publication, July 17, 2022, and in revised form, October 8, 2022 Published, Papers in Press, October 17, 2022,
https://doi.org/10.1016/j.jbc.2022.102606

Nishya Mohamed-Raseek[1], **Cornelius van Galen**[2], **Robert Stanley**[2], **and Anne-Frances Miller**[1,*]

From the [1]*Department of Chemistry, University of Kentucky, Lexington Kentucky, USA;* [2]*Department of Chemistry, Temple University, Philadelphia, Pennsylvania, USA*

Edited by Ruma Banerjee

From the outset, canonical electron transferring flavoproteins (ETFs) earned a reputation for containing modified flavin. We now show that modification occurs in the recently recognized bifurcating (Bf) ETFs as well. In Bf ETFs, the 'electron transfer' (ET) flavin mediates single electron transfer *via* a stable anionic semiquinone state, akin to the FAD of canonical ETFs, whereas a second flavin mediates bifurcation (the Bf FAD). We demonstrate that the ET FAD undergoes transformation to two different modified flavins by a sequence of protein-catalyzed reactions that occurs specifically in the ET site, when the enzyme is maintained at pH 9 in an amine-based buffer. Our optical and mass spectrometric characterizations identify 8-formyl flavin early in the process and 8-amino flavins (8AFs) at later times. The latter have not previously been documented in an ETF to our knowledge. Mass spectrometry of flavin products formed in Tris or bis-tris-aminopropane solutions demonstrates that the source of the amine adduct is the buffer. Stepwise reduction of the 8AF demonstrates that it can explain a charge transfer band observed near 726 nm in Bf ETF, as a complex involving the hydroquinone state of the 8AF in the ET site with the oxidized state of unmodified flavin in the Bf site. This supports the possibility that Bf ETF can populate a conformation enabling direct electron transfer between its two flavins, as has been proposed for cofactors brought together in complexes between ETF and its partner proteins.

Electron transferring flavoproteins (ETFs) were among the first flavoproteins to be discovered (1). They remain notable for the very high one-electron (1e) reduction midpoint potential (E°) of their bound FAD (2) that readily adopts the anionic semiquinone (ASQ) state (3) and thereby shuttles 1e equivalents between various acyl-CoA dehydrogenases and the quinone pool in mitochondria (1, 4, 5). Thus, canonical ETFs serve as diffusible adaptor modules that allow a variety of compounds to contribute to the respiratory electron transfer chain (5). Crystal structures solved for human ETF (*Homo sapiens* ETF, *Hsa*ETF) (6, 7) and canonical ETFs from bacteria (8, 9) reveal a heterodimer in which each subunit contributes a domain to the ETF 'base', which is stabilized by an AMP (Fig. 1) (10, 11). The larger EtfA subunit also contributes most of a third domain that carries the FAD. This 'head' or 'shuttle' domain is tethered to the base by linkers derived from both subunits but has been shown to rotate by some 80 ° in the course of catalytic turnover (12, 13). Thus, the structures captured in crystals fall into two categories. In the 'Open' or 'D' (dehydrogenase-coupled) conformation, the FAD is displayed on the surface and presented to partner dehydrogenases (Fig. S1). In the 'closed' or 'B-like' conformation (bifurcating, *vide infra*), the FAD is partially occluded in the interface between the head and the base. Alternation between conformations is believed to be integral to ETF's catalytic cycle (13, 14) and may gate electron transfer important to the efficiency of electron bifurcation.

The groups of Mayhew, Shiga, and Buckel demonstrated that the ETF of *Megasphaera elsdenii* (*Mel*ETF) contains a second FAD in lieu of AMP (15, 16), accepts a hydride from NADH (16, 17), and mediates electron transfer bifurcation ('bifurcation', Bf) (18). Crystal and cryo-EM structures demonstrated that bifurcating ETFs (Bf ETFs) also stabilize both the open and closed conformations (13, 19–22). Variants retaining only the FAD shared with canonical ETFs demonstrated that this retains the 1e reactivity of canonical ETFs, while the second FAD is the seat of the 2e reactivity that is central to bifurcation (23). Thus, and based on computational replication of the two FADs' distinct optical spectra (23) as well as structural homology (19) and directionality of internal electron transfer (17) and reactivity with NADH (16), it is understood that the FAD shared with canonical ETFs mediates 1e electron transfer (the 'ET' FAD, yellow in Fig. 1), whereas the FAD unique to Bf ETFs that resides in the base mediates bifurcation (the Bf FAD, green in Fig. 1).

The earliest studies found that flavins released from *Mel*ETF included at least three different covalent forms: native FAD, 6-OH FAD, and 8-OH FAD (Scheme S1, (16, 24)). More recently, *Hsa*ETF has been found to accumulate 8-formyl flavin (8fF) (25), making sense of unexpected spectra observed for porcine ETF (26). Since *Hsa*ETF contains FAD only in the ET site, the implication is that the ET FAD is

* For correspondence: Anne-Frances Miller, afmill3r2@gmail.com.
Present address for Nishya Mohamed-Raseek: Institute of Biological Chemistry, Washington State University, Pullman WA 99164.

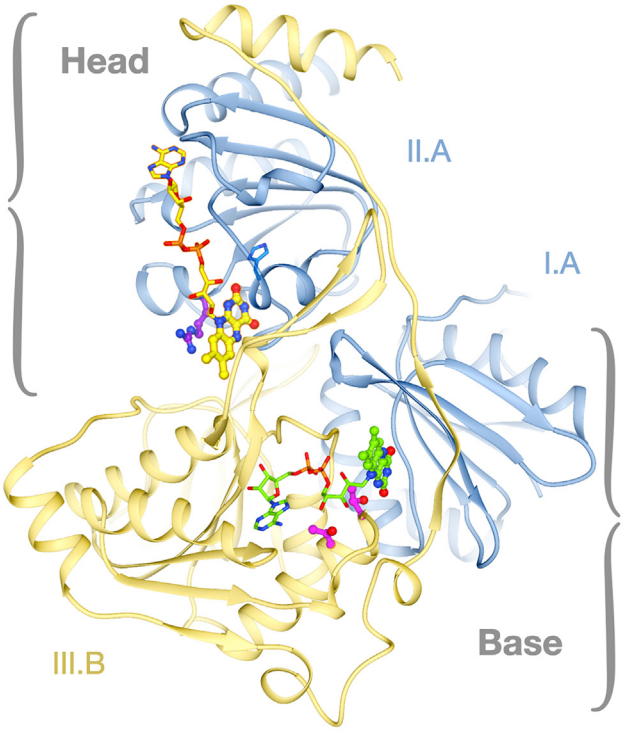

Figure 1. Ribbon diagram of a Bf ETF heterodimer. Its structure in the closed conformation is shown with the EtfA subunit in *blue* (domains I.A and II.A) and the EtfB subunit in *gold* (domain III.B). Although ETF is made up of three domains, domain II.A from EtfA moves relative to the other two (12, 13) so the structure is often discussed in terms of two structural units, the larger of which is comprised of domains I.A and III.B. This 'base' is in the *lower portion* of the figure and contains the Bf FAD (*green*) with its flavin moiety at the interface between the contributing domains I.A and III.B. The 'head' or shuttle domain (above) is comprised mainly of domain II.A from the A subunit and contains the ET FAD (*yellow*). Base residues in *pink* were mutated to prevent binding of the Bf FAD (Thr-94.B and Thr-97.B, in the numbering of *Rhodopseudomonas palustris* ETF, *Rpa*ETF (23)). The head's Arg-273.A (in *purple*) has been shown to modulate the reduction midpoint potentials (E°s) of the ET FAD (38).

unusually susceptible to modification. We suspect that this may be related to the unusual degree to which the flavin ASQ state is stabilized by this site.

A stable SQ state of the flavin is essential to bifurcating ETFs' activity, because it enables the ET flavin to perform 1e transfer. Electron transfer bifurcation ('bifurcation') in ETFs involves acceptance of a pair of electrons as hydride from NADH followed by transfer of one to a higher-E° acceptor and the other to a lower-E° acceptor, thereby generating a reductant that is more powerful than NADH. The lower-E° products, reduced ferredoxin or flavodoxin, both support critical reactions such as N_2 fixation (27). Bifurcation is thermodynamically allowed only because production of the low-E° product is coupled to favorable reduction of a high-E° carrier. However, the efficiency of bifurcation rests critically on a gate that allows only one of the two electrons to pass to high E°. Alternation of conformations has been proposed to enforce this (13) but still requires that the ET flavin accept electrons only one at a time. This in turn requires that a semiquinone state be strongly stabilized, in contrast to the case for free flavin (28). Moreover, if ET flavin's resting state *in vivo* is the ASQ state, then it will only have capacity to accept a single electron (29, 30). This would force the high-energy electron to pass to the low-E° acceptor instead, even in the absence of a conformational gate (31). Thus, the unusual redox tuning of the ET flavin is central to Bf ETF's mechanism, motivating us to better understand this reactivity as a whole, including ET flavin's heightened tendency to covalent modification.

Our exemplar of Bf ETFs is the ETF from the nitrogen-fixing phototroph *Rhodopseudomonas palustris*, *Rpa*ETF (32). To compare this with a model canonical ETF that differs in as few respects as possible, the T94,97A variant was used. In this, both Thr-94 and Thr-97 of the smaller (B) subunit were replaced by Ala, thereby eliminating two hydrogen bonds that stabilize the flavin-proximate phosphate of FAD. T94,97A-*Rpa*ETF possesses AMP in place of the Bf flavin, similar to canonical ETFs, and its ET flavin displays the 1e redox reactivity with stable ASQ that typify canonical ETFs, with a relatively high oxidized/anionic semiquinone (OX/ASQ) reduction midpoint potential, $E°_{OX/ASQ}$, of -7 mV (23). Crucially, the Thr to Ala substitutions that weaken Bf FAD binding do so without directly perturbing the interface between subunits or the ET site, so effects on the ET flavin will be indirect only. Moreover, the Thr to Ala substitutions convert residue identities conserved among Bf ETFs to identities more common among canonical ETFs (33). Thus, our T94,97A variant constitutes a model for canonical ETFs that is otherwise almost identical to the Bf *Rpa*ETF, facilitating direct comparison between the two types.

Our *Rpa*ETF-derived canonical model duplicates the oxidation of the ET flavin 8-methyl to a formyl group found by (25), but in extending our investigation to the Bf ETF containing two FADs, and anaerobic conditions more typical *in-vivo*, we demonstrate formation of a further modified flavin. We show that the special environment of the ET site potentiates the bound flavin for displacement of its 8-methyl by a fragment derived from our amine-based buffer. Tris buffer was found to stimulate modification of a flavin in another case (34) but this is the first instance we are aware of where portions of the buffer molecule become incorporated into the modified flavin product. The resulting species succeeds in explaining a perplexing signal observed near 726 nm (35), in terms of a charge transfer complex suggesting conformational change within an ETF or association of two ETFs that brings their flavins together.

Results

Formation of 8fF confirmed, in air

Working at pH 8 in air, Augustin *et al* found that certain amino acid substitutions caused human ETF (*Hsa*ETF) to accumulate a modified flavin that they demonstrated to be 8fF (25). Accumulation was slower at pH 7 and in the WT *Hsa*ETF. Similarly, we found that WT *Rpa*ETF did not accumulate significant 8fF at pH 8, but it gradually accumulated modified flavin at pH 9. Accumulation was accelerated in the T94,97A variant possessing only the ET flavin. Therefore, and

because it is a simpler system, we began with T94,97A-*Rpa*ETF.

Figure 2*A* shows the optical spectrum of T94,97A-*Rpa*ETF at the completion of purification and concentration in pH 9 buffer *versus* 24 h later. Spectra of material purified into pH 8 *versus* pH 9 revealed that at pH 9, changes occurred in the hour required for buffer exchange on a desalting column followed by concentration by ultrafiltration. However, samples prepared and held at pH 8 showed no change for days. Moreover purification steps prior to buffer exchange were always conducted at a lower pH. Thus, the pH 8 preparation can be taken to represent absence of modification (Fig. 2*A*). Spectra of flavins released from material purified into pH 9 demonstrate that the spectral changes reside in the flavin itself (Fig. 2*B*). Flavin released after purification at pH 9 displayed characteristics of 8fF including a blue-shifted band II (with λ_{max} near 360 nm) and strength comparable to that of band I (near 450 nm) (25) (Fig. 2*B*, blue trace). This contrasts with the weaker, longer-wavelength band II of authentic FAD near 374 nm. For flavin released from samples held at pH 9 for 24 h, a stronger-than-expected amplitude for band I with a shoulder at longer wavelengths suggested the presence of an additional modified FAD (*vide infra*), but the dominant spectral changes were suggestive of oxidation of the 8-methyl group to a formyl group (this C atom is denoted as C8M, Scheme S1).

To test for 8fF, released cofactors were characterized by electrospray ionization mass spectrometry (ESI-MS) in anion mode (ES-). The mass spectrum of cofactor from T94,97A-*Rpa*ETF held at pH 9 displayed a prominent peak corresponding to authentic FAD at 784 m/z, accompanied by another strong peak at m/z = 822, as expected for 8fF complexed with a Na^+ ion (Fig. S2). In contrast, only the m/z = 784 peak was found in the mass spectrum of flavins from WT-*Rpa*ETF purified at pH 8. This confirms oxidation of a methyl to a formyl group in the FAD in T94,97A-*Rpa*ETF. Two methyls are present in FAD, but the one at position 8 is much more reactive (36, 37). Thus, the rapid modification of the flavin of T94,97A-*Rpa*ETF at pH 9 is attributable primarily to formation of 8fF, as in *Hsa*ETF (25).

8fF occurs in the ET site yet is responsive to the Bf site

8fF formation also explains the sharp feature that grew into T94,97A-*Rpa*ETF's optical spectrum at 432 nm, as well as the long-wavelength absorption extending beyond 700 nm (Fig. 2*A*). Both are attributable to 8fF in the ASQ state (25). Thus, bound 8fF's $E^\circ_{OX/ASQ}$ appears sufficiently high that the ASQ can form even in air-equilibrated buffers, as in (2). Upon release from the protein, the 8fF returned to the OX state, based on disappearance of both these features, indicating that the $E^\circ_{OX/ASQ}$ is elevated by interactions in the ET site. This replicates the effect of the ET site on authentic FAD, which experiences greatly enhanced stabilization of the ASQ state when bound in the ET site (38, 39–41). Similarly, the flavin optical spectrum when bound differs from that when free, confirming that 8fF experiences a distinct environment when bound in the ET site. The fact that 8fF forms only when FAD is bound suggests that the peculiar environment provided by the ET site activates the flavin for modification.

The fact that 8fF is formed in our T94,97A variant that only contains the ET flavin is consistent with modification of FAD in *Hsa*ETF that also lacks a Bf flavin (25). However, even in WT-*Rpa*ETF containing two FADs, modified flavin did not exceed half of the total after the content of modified FAD had ceased to change. Treatment with ADP confirmed that only the ET FAD was modified (42). Presence of the second FAD nevertheless affected the pace of the process, as the rate of 8fF formation was faster in T94,97A-*Rpa*ETF than in Bf FAD-containing WT-*Rpa*ETF. This was also true for the R165H-*Rpa*ETF, another variant that also abrogates Bf FAD binding. These amino acid substitutions are all distant from the ET site, in a different domain and subunit of the protein (Fig. 1) (38),

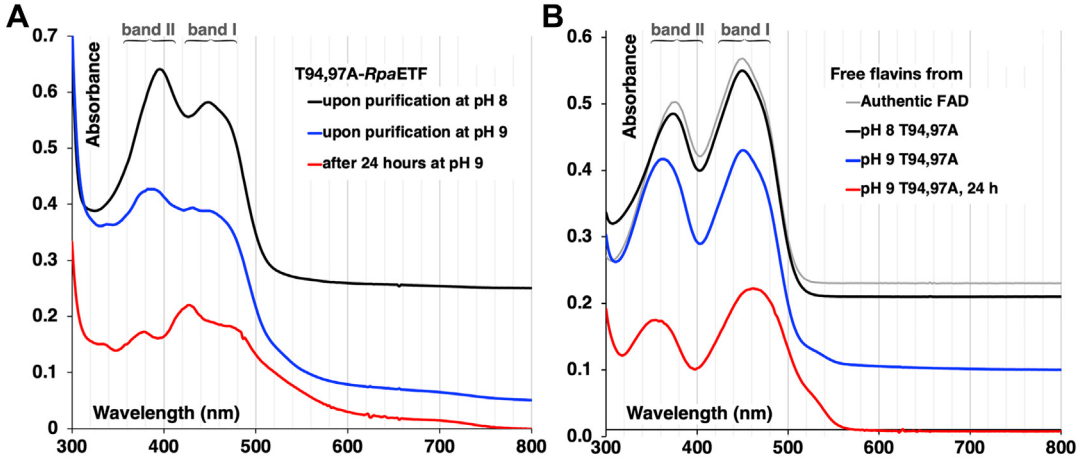

Figure 2. Spontaneous conversion of T94,97A-*Rpa*ETF at pH 9. Panel *A* compares visible spectra of T94,97A-*Rpa*ETF purified into buffer at pH 8 or 9. *Black*: pH 8 control which is unchanged over weeks. *Blue*: T94,97A-*Rpa*ETF purified by same protocol but transferred into pH 9 buffer instead of pH 8 following the CoNTA column, approximately an hour after initial exposure to pH 9. *Red*: replicate pH 9 sample 24 h later (held at 4 °C in darkness at pH 9). Panel *B* compares spectra of flavins released from the proteins in panel *A*. *Black*: flavin released from T94,97A-*Rpa*ETF freshly purified into pH 8, *blue*: flavins released from T94,97A-*Rpa*ETF freshly purified into pH 9, *red*: flavins released from T94,97A-*Rpa*ETF held for 24 h at pH 9, *gray*: authentic FAD control. Sample concentrations were 30 μM, please see the Methods for CoNTA chromatography. CoNTA, co-nitrilotriacetate.

so perhaps the presence of Bf FAD slows modification by favoring the closed conformation that seems less prone to ET flavin modification (25). Overall, the modification affects only one of the two FADs and so can be attributed to reactivity conferred on the ET flavin by its binding site.

Influence of amino acid substitutions

Accelerated modification at pH 9 *versus* at pH 8 is consistent with mechanisms of 8fF formation that invoke deprotonation of the 8-methyl to form a methide intermediate (37, 43, 44) and/or nucleophilic attack at the 8-methyl by HO^- (45) (Scheme S2). These mechanisms imply that stabilization of an anionic state of the flavin should favor 8fF formation, as has been demonstrated in the FOX enzyme (43, 46) and *Hsa*ETF (25). In *Rpa*ETF, the conserved Arg-273 that is adjacent to the ET flavin has been shown to stabilize the anionic ASQ of the flavin (38) as in canonical ETFs (39, 41). Therefore, we tested the possibility that flavin modification occurs *via* a stabilized anionic intermediate, by replacing Arg-273. Substitution by either Ala or His essentially eliminated modification of the flavin, whereas the control R273K variant that retains positive charge underwent flavin modification as for the WT (Fig. S3). This is consistent with protein-site stimulated formation of 8fF *via* either (1) a negatively charged intermediate (2), the deprotonated state of a nearby base, and/or (3) direct participation of HO^-.

A reductive reaction is confirmed in the absence of O_2

Literature mechanisms for formation of 8fF call for oxidation of intermediates by O_2 (Scheme S2) (43, 45, 47). Nevertheless, anaerobic incubations of *Rpa*ETF produced the same modified flavins as did aerobic incubations, although the timescales differed, requiring the use of WT-*Rpa*ETF for reasons of stability.

Anaerobic reactions displayed a loss of approximately half the optical signal intensity, whereas overall absorbance changed very little in air (Fig. 3). This suggests reduction of one of *Rpa*ETF's two flavins, as also seen in other enzymes where a flavin gets modified (47, 48). The retained OX flavin spectrum in the anaerobic reaction resembled that of Bf flavin based on the λ_{max} values and unresolved vibronic structure (38), indicating reduction of the ET flavin. In the same time interval, the aerobic reaction's signals changed shape, gaining new intensity between 500 and 550 nm, and near 320 nm, consistent with conversion of one flavin to 8fF (absorption maxima of free OX state near 352 and 463 *vs.* those of authentic FAD near 375 and 450 (26) and 8fF ASQ can explain the absorbance seen near 430 nm). Since this is seen only in aerobic reactions, we attribute it to the ET flavin, consistent with the behavior of T94,97A-*Rpa*ETF, above. The anaerobic reaction medium did not provide exogenous reductants, but reduction of the ET flavin isoalloxazine ring system is consistent with its serving as an electron sink for oxidation of the 8M methyl group.

In both aerobic and anaerobic reactions, the Bf flavin remained OX even after 216 h, consistent with the low E°, expected if this flavin remains unmodified. However, spectra collected at the longest times reveal a sharp feature near 355 nm in anaerobic reactions (Fig. 3*B*). We attribute this to the hydroquinone (HQ) state of a modified flavin in the ET site since it is absent from spectra of air-equilibrated samples at comparable times and by analogy with a very similar feature at 340 nm demonstrated for 8fF by Augustin *et al.* (25). Moreover, the presence of an additional modified flavin (other than 8fF) is supported by absorbance in aerobic reactions at wavelengths longer than 510 nm, where even 8fF does not significantly absorb.

Spectra from the aerobic reaction revealed a second phase in which band II shrank but band I's component at long wavelengths completed its growth. This second event could also

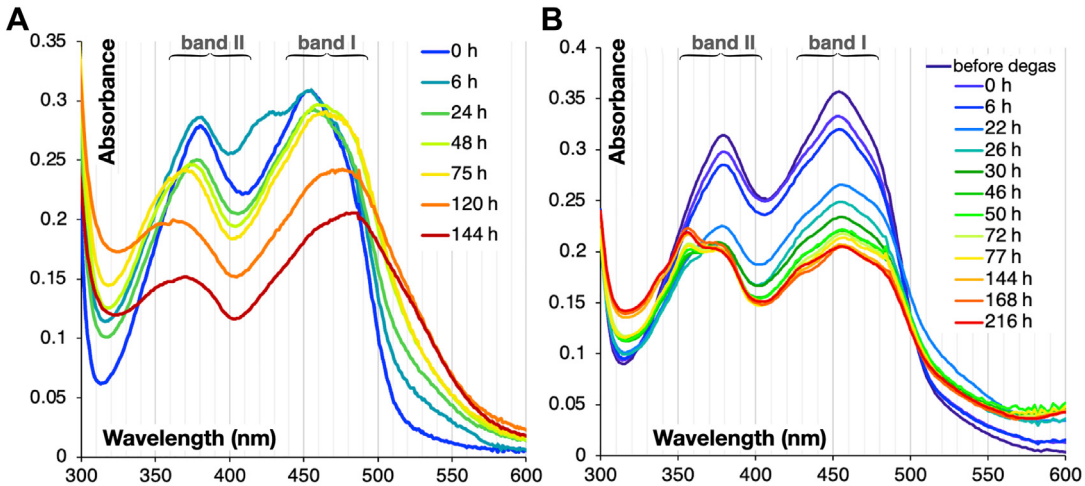

Figure 3. Comparison of visible spectral changes as a function of time in aerobic *versus* anaerobic WT-*Rpa*ETF at pH 9. *A*, a 220 μM sample was held in darkness at 4 °C at pH 9 and aliquots were withdrawn and diluted aerobically to 14 μM in more of the same pH 9 buffer for collection of the absorbance spectra shown here. *B*, a 370 μM sample was held anaerobically in darkness at 4 °C at pH 9; aliquots were withdrawn and diluted anaerobically to 14 μM in the same buffer and the spectra were also collected without exposure to air, within the anaerobic chamber. Times of 120 h, 144 h, 168 h, and 216 h correspond to 5, 6, 7, and 9 days, respectively and are ± 1 h.

occur in the anaerobic reaction but be inconspicuous if it affects the flavin that is reduced. To test for additional reaction after formation of 8fF, samples withdrawn at various times were denatured by heating, and released flavins were observed after oxidation.

Released flavins confirm a second product

Over 3 days' aerobic reaction, released cofactors' band II shifted to shorter wavelengths and became stronger than band I, which shifted to longer wavelengths, consistent with 8fF formation (yellow spectrum, Fig. 4*A*). A quasi-isosbestic near 480 nm indicates that spectral changes reflect predominantly a single conversion. At later times, band II shifted back to longer wavelengths and lost intensity, confirming that an additional reaction consumed 8fF. This second phase was also marked by growth in 525 nm intensity, confirming the 525 nm species as a later product than 8fF. No additional species was observed even over weeks, indicating that the 525 nm species is a terminal product and making 8fF an intermediate.

Flavins released from anaerobic reactions did not display accumulation and then consumption of 8fF intermediate. Although an early quasi-isosbestic near 480 nm can still be seen (Fig. 4*B*), the long-term product appeared without significant delay or shift in Band II. This proved to reflect use of higher ETF concentrations in anaerobic reactions, as consumption of 8fF was also accelerated in more concentrated aerobic samples (Fig. S4), masking early formation of 8fF. Because spectra of released flavins indicated comparable reaction trajectories in anaerobic and aerobic reactions of 350 μM *Rpa*ETF, and the same final product was obtained, we argue that O_2 is not essential for conversion of 8fF to the later product.

Involvement of buffer in modification of flavin

Because the concentrated anaerobic reaction yielded a single product flavin with fewer possible complications from intermediate forms, we used these conditions to generate the long-term product for characterization. Deconvolution of the spectrum of the final mixture of released flavins reveals that one of *Rpa*ETF's flavins was not modified (Fig. 4*C*), the Bf flavin based on the experiments above. The deduced spectrum of the modified flavin that formed is shown (red spectrum in 4C). The similarity between this spectrum and those of 8-amino flavin (8AF, λ_{max} =479–499 nm) (45, 47) and roseoflavin (= 8-dimethyl amino flavin, λ_{max} =488–500 nm) (49) suggested that the ET flavin acquired an amine functionality at the 8 position (Scheme S1). Modifications at position 8 by either OH or SH also produce a single dominant band at $\lambda >$ 450 nm (50–52); however, neither is compatible with our adduct's formation in ≤2 days in the presence of amine-based buffers, but not in their absence. Our 8AF-like spectrum recalls the result that 8fF is an on-pathway intermediate in the enzymatic formation of 8AF and then roseoflavin by RosB (47), suggesting that the ET site of *Rpa*ETF may replicate reactions catalyzed by RosB. Whereas glutamate was identified as the source of the amine installed by RosB (47), the most abundant amine in our system is the buffer: 1,3-bis[tris(hydroxymethyl) amino]propane (BTP, Scheme S1). Moreover, at the pH of 9 we used, compared to BTP's lower pK_a of 6.8, one of the

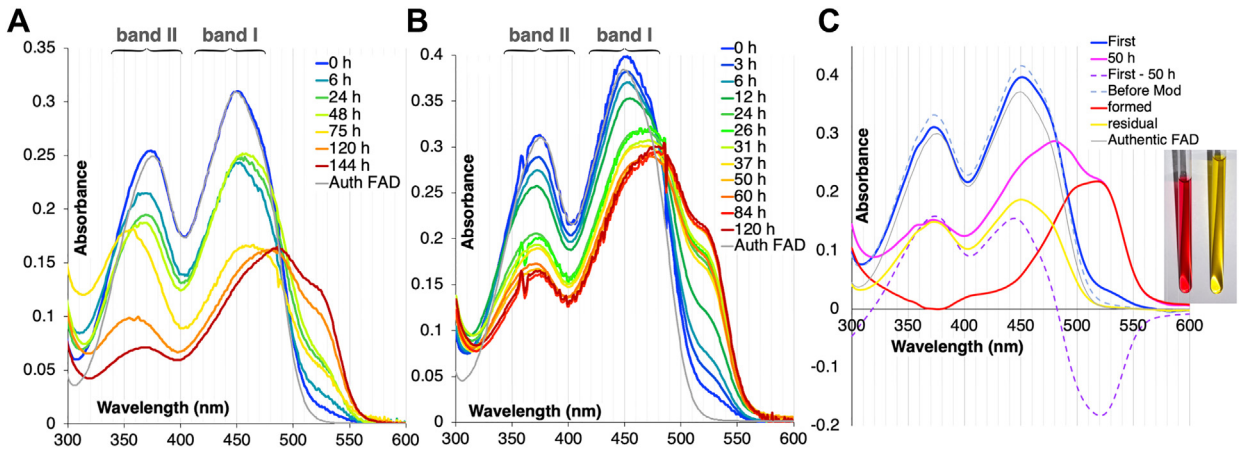

Figure 4. Flavins formed in aerobic and anaerobic reactions. Flavins released from aerobic reaction of 224 μM *Rpa*ETF (*A*) *versus* anaerobic reaction of 345 μM *Rpa*ETF (*B*) and compared with deconvoluted optical spectra of flavins formed (*C*). For each reaction, aliquots were removed at the indicated times and treated to release the flavins from the protein (see Experimental procedures). Spectra shown are scaled to 14 μM, 18 μM, and 18 μM *Rpa*ETF, respectively. The precipitated protein pellets were all colorless, indicating that no flavin was lost with the protein. Based on spectra of released flavins, the initial time points of the reactions were dominated by unmodified FAD. In panel *C*, spectra of the first sample of released flavins (called 0 h in panel *B*) and of flavins released from a sample reacted for 50 h are shown. The *purple dashed* difference spectrum representing the reverse of the conversion that occurred over 50 h was used to correct the first spectrum for the signature of 8AF already present around 525 nm. This amounted to approximately 10% of one flavin's worth of 8AF and yielded the idealized 'Before Mod' spectrum, corresponding to the spectrum before any modification had occurred (*pale blue dashed line*). This spectrum representing 2.0 FADs was subtracted from the 50 h spectrum after multiplication by 0.45 to yield a fully positive difference spectrum, shown in *red*. This is the absorbance not explainable by FAD and therefore representing the formed flavin (*red* = *pink* minus 0.45 **dashed-blue*). The spectrum of the 0.9 flavins subtracted is in *yellow* and labeled 'residual' since it is the difference between the observed spectrum of flavins released after 50 h (*pink*) and the spectrum attributed to modified flavin (*red*). Spectra of authentic FAD are provided in *gray* in each panel, for comparison. Inset: photo of NMR samples. Authentic FAD was purchased from Chem-Impex International and dissolved in ^2H_2O (*yellow*), the precipitated flavins released from a 50 h anaerobic reaction of *Rpa*ETF were dissolved in ^2H_2O to yield the *red* sample.

secondary amines would be deprotonated and could commit a nucleophilic reductive attack on 8fF.

To learn if amine buffers can contribute an amine functionality to the flavin, we analyzed the red flavin by ESI-MS. To isolate the modified flavin, the mixture of released flavins was allowed to sit in darkness at 4 °C. Red flavin precipitated leaving a yellow supernatant whose spectrum was indistinguishable from FAD's. When red precipitate was redissolved in water, its spectrum accounted for the one that grew in the course of reactions (compare with figures below). This precipitate was therefore analyzed by ESI-MS and yielded MS fragments compatible with a BTP-flavin adduct (Fig. 5). When *Rpa*ETF reacted anaerobically in a buffer of Tris (tris(hydroxymethyl)aminomethane) instead of BTP, a red flavin was again obtained. However, it produced different MS fragments, compatible with a Tris-flavin adduct (Fig. 5).

Specifically, authentic FAD, the product of reaction in Tris, and the product of reaction in BTP all produced the fragments expected from the adenine containing portion of FAD (53), and the expected companion product is observed from FAD at 255 Da (corresponding to lumiflavin, LF). However, the Tris product and the BTP product each produced different companion fragments that were larger, different from one-another, but both explainable by the structure of the parent buffer. The Tris product displayed a fragment at 384 Da consistent with a Tris-LF adduct complexed with Na^+ counterion (361 + 23 Da). BTP product included a peak at 849 Da consistent with the adduct of part of BTP with FAD shown in the figure, in complex with Na^+ (826 + 23). An additional prominent fragment at 504 can be explained by loss of an O atom from an OH of BTP attached to LF (520–16 Da, structures not shown) as can the peak at 402 Da (see Fig. S5). Thus, it appears that amine buffers contribute an N-containing fragment to the red flavin mass spectrum, although the precise identity of the fragment retained is obscured by the variety of fragments produced in MS. The visible spectrum, in conjunction with NMR demonstrating retention of only one methyl group, agrees with known reactivity in arguing that the amine is attached in place of the 8-methyl of FAD.

Since both amine-based buffers produced flavins whose spectra resemble 8AF and roseoflavin (45, 54, 55) and the one formed in BTP lost a methyl group based on NMR, we infer that both are 8AFs, with the identity of the attached amine depending on the buffer from which it was derived. This is supported by the pH dependence of the red flavin's optical spectrum (Fig. S6), which resembles those of 8-OH and 8-SH flavins (50–52). We adopt the notation 8AF in a generic sense to indicate this product of reaction with BTP in what follows, as well as the product formed from Tris, while recognizing that the precise nature of the substituents attached to the amine N depends on the reaction conditions.

Intermediacy of a radical and improved understanding of a long-wavelength band

Even though our reactions were conducted in darkness to minimize photoexcitation of flavin, anaerobic incubation resulted in flavin reduction and the buffer is a possible electron donor. Therefore, we sought to identify the reduced flavin state. Examination anaerobic reactions at wavelengths beyond 600 nm revealed growth of a strong band at 726 nm. Indeed, the sample became olive green in color. The long-wavelength signal has been correlated with formation of the HQ of ET flavin (ET-HQ) in the presence of OX Bf flavin (Bf-OX (35), Fig. 6*A*) and attributed to a charge-transfer (CT) complex of ET-HQ • Bf-OX (35). However, this would require the two flavins to make van der Waals contact with one-another, which has not been observed in any ETF crystal structure. Therefore, we sought to test an alternative possibility: that the 726 nm band might correspond to an SQ state of modified flavin in the ET site. Long-wavelength bands are well known for flavin SQ states (56). In particular, the neutral SQ state of 8fF semiquinone has excitation maxima at wavelengths greater than 600 nm (25, 26, 57).

Figure 6*B* compares the EPR spectra obtained at room temperature for aliquots withdrawn at different times from anaerobic reaction of *Rpa*ETF in pH 9 BTP. An EPR signal was indeed observed. Early in the reaction, the peak-to-trough width was 10 G, consistent with a population dominated by 8fF (58). However, the later signals displayed peak-to-trough widths of 12 G, indicating that a different radical species attains dominance, analogous to the conversions observed optically. This broader signal is still narrower than that of FAD ASQ (at 15 G (59, 60)) but more similar to the 12 G width reported for flavin linked *via* C8M to a His side chain (61).

At maximum, the EPR signal accounted for a spin population of 0.16 (most likely, *Rpa*ETF containing one radical accounts for 16% of the population). This occurred long before the 726 nm signal had attained full strength, and indeed, the radical population shrank as the 726 nm band grew, at long times (Fig. 6*D*). Since the radical was formed by reduction of OX flavin, as indicated by diminishing absorbance at 455 nm, the later diminution of radical is most simply attributed to further reduction to HQ. This is consistent with the published attribution of the 726 nm signal to a species containing a HQ state of one flavin and the OX state of another (35). It is also consistent with accumulation of a signal attributable to modified flavin HQ near 355 nm, at times later than 72 h (3 days) (Fig. 6*A*).

Because the radical population was small throughout, it can be a consequence of formation of 8fF and the fact that the $E^{\circ}_{OX/ASQ}$ of 8fF is higher than that of FAD (2, 3). Its maximum coincided with completion of the formation of 8AF based on A_{525} of released flavin and suggests that broadening of the EPR signal reflects conversion of 8fF to 8AF (possibly *via* unresolved intermediates, Fig. 6*B*). At longer times, the 726 nm band continued to grow, suggesting a slow step following formation of 8AF. This was not accompanied by any further change in the chemical composition of flavins based on their spectra after release (Fig. 6*C*) and only very slight changes in the population of OX flavin based on absorbance at 455 nm (Fig. 6*D*), so we speculate that it could reflect a conformational change or dimerization bringing two flavins sufficiently close together to produce a CT complex. The sequence of events

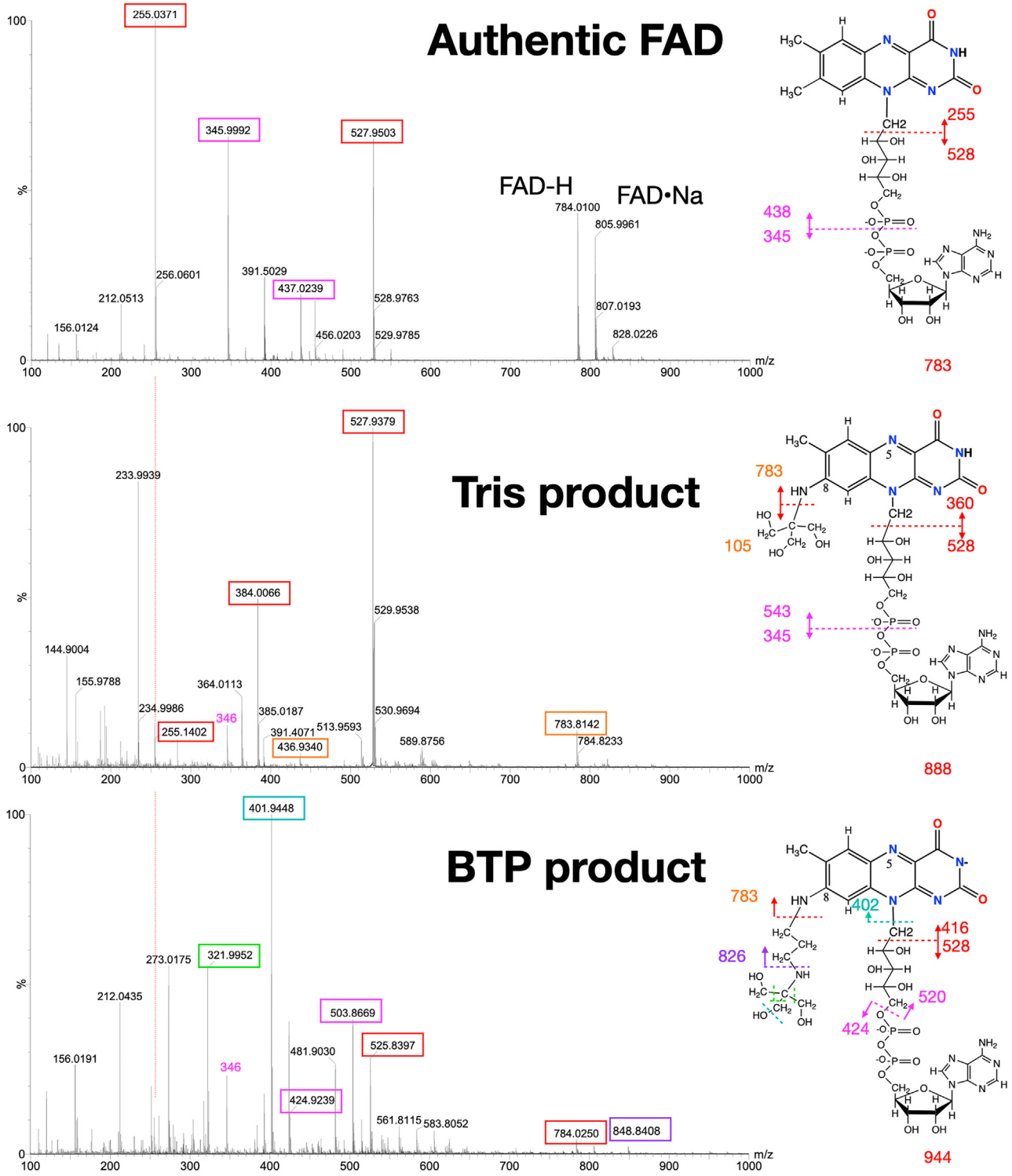

Figure 5. Mass spectrometric identification of red precipitates as adducts of flavin and buffer fragments, based on ESI MS of flavins formed anaerobically in WT-*Rpa*ETF. The *top panel* shows authentic FAD. The *middle panel* shows flavin released from a sample held in pH 9 Tris buffer, wherein the ADP fragment at 528 Da is unchanged but the 255 Da fragment corresponding to lumiflavin is lost and replaced by a new fragment at 384 Da, which is explainable as a Tris-flavin adduct complexed with Na^+ (*red dashed lines*). The *lower panel* shows flavin released from a sample held in pH 9 BTP buffer, wherein the 528 Da fragment is retained but different flavin-containing fragments are seen, demonstrating that the buffer identify affects the product identity. BTP, 1,3-bis[tris(hydroxymethyl)amino]propane; ETF, electron transfer flavoprotein; ESI-MS, electrospray ionization mass spectrometry.

indicates that 8AF formation is a prerequisite for 726 nm band formation. We therefore tested whether it might even be sufficient, upon partial reduction.

Nature of the 726 nm species

The attribution of the signal near 726 nm to CT between the HQ of one flavin and the OX state of another was supported

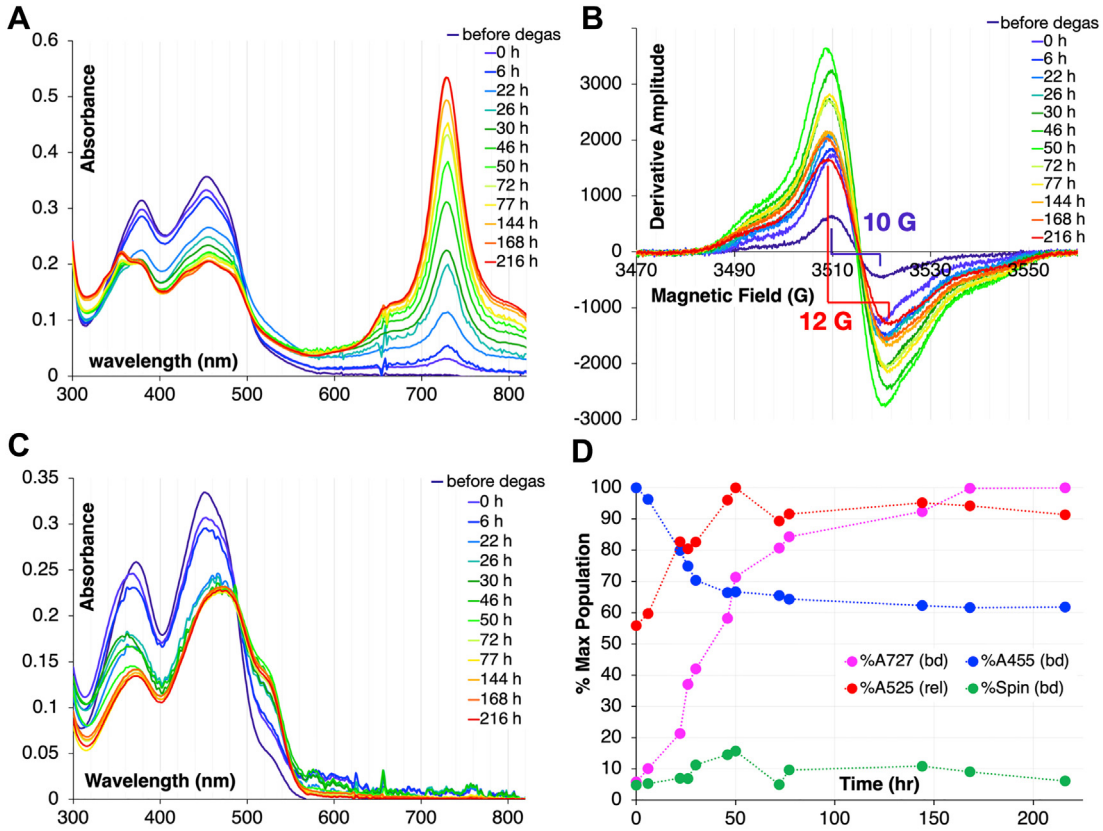

Figure 6. Time course of anaerobic reaction as documented by visible absorption and EPR spectra of bound flavins, and visible absorption spectra of oxidized reseased flavins. Time course of anaerobic reaction as profiled by visible spectra (*A*), EPR spectra (*B*), and visible spectra of OX released flavins (*C*), with comparison of timing of different changes (*D*). In all cases, the 0 h time point is at the end of the degassing interval under inert atmosphere. 370 μM *Rpa*ETF was allowed to react anaerobically in darkness at 4 °C and samples were used at that concentration for EPR (panel B), diluted to 14 μM for collection of absorption spectra (panel *A*) or diluted approximately 26 fold in the course of removing protein (panel *C*). Panel *B* shows that some 5% of sites undergo 1e reduction in this interval, consistent with Figure 3*B*. In panel *D*, amplitudes for flavins released from *Rpa*ETF are denoted by 'rel' and corrected for dilutions used in releasing the flavin. The other amplitudes reflect intact *Rpa*ETF and are denoted by 'bd' for 'bound'. The EPR signal strengths were converted to spin concentrations responsible for plotting in panel *D*. Similarly, the initial amplitude at 455 nm was attributed to two OX flavins, so its eventual decrease to 60% amplitude indicates that one of the two flavins underwent reduction to a state with low but non-zero absorbance at that wavelength (HQ). A_{525} values are reported as % of the maximal value observed at 50 h; we do not consider the apparent drop in signal at longer times to be significant. The maximal signal at 525 was attributed to one equivalent of flavin because one equivalent of unmodified flavin remained when A_{525} had leveled off at its terminal value (only one of the two flavins per *Rpa*ETF was modified). The amplitude of A_{727} is likewise presented as a % of the maximal value observed. EPR, electron paramagnetic resonance.

computationally (35) and rests on literature precedent, as such bands have been characterized even for free FMN (62). Indeed, free 8AF in pH 9 BTP formed such band upon partial reduction, but with an absorption maximum of 717 nm, rather than the 726 nm observed in protein (Fig. 7*A*). Further reduction abolished the band, as in *Rpa*ETF. Thus, the protein is not required for formation of the CT species.

Our titrations were performed at a lower free flavin concentration than those of earlier authors (62, 63), indicating that our 8AF has a higher tendency to dimerize. This is consistent with the 717 nm band's narrower width and distinct features suggesting a better defined or longer lived complex, despite the absence of protein. Given that the diphosphate groups of the two FAD variants would repel one-another, we wondered whether our use of a buffer with two potentially cationic sites was significant, and whether once again, BTP might be noninnocent.

To determine whether BTP at pH 9 is required for formation of the presumed CT complex, we performed a reductive titration in its absence. 8AF in water at pH 6.8 was reduced stepwise (Fig. 7*B*). Between 300 and 550 nm, the spectra resembled what was seen in 20 mM BTP. The sharp signal that formed near 320 nm is attributed to the HQ state of 8AF because it formed upon full reduction. This substantiates our assignment to a modified flavin HQ of the similar sharp 340 nm feature observed in modified *Rpa*ETF (Fig. 3*B*).

In water, a CT band formed half-way through reduction. However, it was broad and featureless, resembling the more commonly observed flavin CT bands (62–64). Crucially, the featureless band could be converted to the sharper better-defined 717 nm band by simple anaerobic addition of BTP (Fig. 7*C*). The elevation of pH that likely accompanied addition of BTP might also contribute to the spectral changes. Fig. S6 shows that deprotonation of the 8AF shifts intensity from a component at 490 nm to one at 570 nm and produces better-defined features. However, considering the electrostatics attending FAD and BTP, it seems likely that BTP also interacts with the participating flavins' pyrophosphates, and we credit

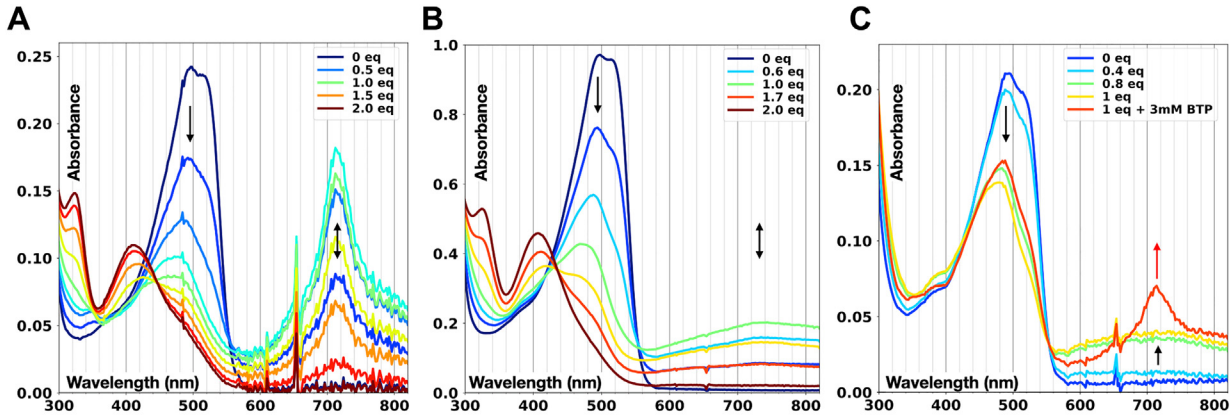

Figure 7. Reductive titrations of 8AF produced in BTP. *A*, the *red* precipitate was redissolved in 20 mM BTP and reduced with small aliquots of Ti citrate. The legend provides number of reducing equivalents present at selected points. *B*, as in (*A*) but the precipitate was redissolved in water. *C*, as in (*B*) to midway through the reductive titration, at which point 20 mM BTP (pH 9) was added to yield a final concentration of 3 mM. The total flavin concentrations were 27.3, 111.6, and 22.85 μM, respectively. Note the excellent agreement between the initial spectrum in (*A*) and the spectrum deduced by deconvolution in Figure 4*C*.

that with suppressing structural fluctuations and transient dissociations that cause line broadening in BTP's absence. Collectively, our data demonstrate that 8AF and partial reduction are necessary, and along with BTP are sufficient, to form the strong, featured CT species observed near 720 nm.

Because the distinctive CT band is formed from 8AF, we infer that 8AF was present in the *Rpa*ETF that displays the 726 nm band. We attribute it to bound rather than released flavin, because the samples contained 2 FAD per ETF and did not display the precipitation that inevitably accompanies flavin release from *Rpa*ETF. Together, our data argue against the possibility that our enzymes contained a precursor, representing a committed intermediate that advances to 8fF and 8AF only upon exposure to air during flavin release.

Our initial report proposed that the 726 nm band reflects reduced ET flavin in complex with OX Bf flavin, and our current data suggest that the ET flavin was most likely 8AF while the Bf flavin remained FAD (compare Fig. 8*A* of Duan *et al* (35) with the red trace in Fig. 4*C*, above). Thus, in retrospect, the proposed CT complex between the ET flavin and the Bf flavin would have contained the HQ of 8AF in complex with the OX state of authentic FAD. However, our new data reveal that 8AF alone can produce such a band at 717 nm.

To test the possibility of a CT complex between 8AF-HQ and FAD-OX, we mixed equal quantities of 8AF and FAD and conducted anaerobic stepwise reduction of the mixture (Fig. 8*A*). Two reductive phases were seen, corresponding to formation of the CT followed by its disappearance (difference spectra describing each phase are shown in Fig. S7). The first phase displayed a clear isosbestic indicating that a single process dominated and the difference spectrum associated with phase 1 revealed loss of the oxidized spectrum of 8AF with the formation of 8AF-HQ (shoulder at 350), in conjunction with growth of CT intensity at 717 nm (compare Fig. S7*A* dark teal difference with 8AF spectrum in Fig. 8*A*). The inset demonstrates linear relationship between reduction of 8AF and formation of 717 nm band (Fig. 8*A* inset).

After completion of phase 1, the spectrum between 300 and 500 nm was dominated by that of OX FAD (lime green in Fig. 8*A*), which also underwent 2e reduction without significant population of an intermediate. The difference spectrum associated with phase 2 revealed loss of the 717 nm band in conjunction with reduction of FAD-OX to the corresponding HQ (Fig. S7*A*). The fact that the 717 nm band grows with reduction of one flavin and then decays with reduction of the second flavin demonstrates that the band emanates from two flavins rather than a flavin and its attached adenine. This experiment also rules out the possibility that the 717 nm band represents SQ of the 8AF, which would have been maximal half-way through reduction of 8AF. Instead, the 717 nm signal is maximal at the halfway point of the titration of both flavins (1.0 reducing equivalent relative to the total concentration of flavins) when the spectrum shows that the FAD remains oxidized whereas the 8AF is fully reduced. This is in contrast with the interpretation of the half-reduced spectrum of 8-mercaptoFMN in (65). Thus, the 717 nm band represents 8AF-HQ in complex with FAD-OX.

Panel B shows that when only 8AF is present, the 300 to 550 nm spectrum half-way through the reduction is recognizably a mixture of the OX starting spectrum and the final HQ spectrum. However, in the region of $\lambda > 600$ nm, the spectrum half-way through reduction cannot be constructed by any linear combination of the starting and ending spectra. This demonstrates formation of a distinct chromophore when OX and HQ 8AF coexist. Interestingly, the CT band formed by 8AF-HQ • FAD-OX has the same λ_{max} of 717 nm as that of 8AF alone (Fig. 7). This insensitivity to composition is somewhat surprising given that Abramovitz and Massey saw CT band wavelengths trend with the separation between the E°'s of the donor and the acceptor (66). It also prevents us from inferring whether the band seen in *Rpa*ETF corresponds to a complex of $(8AF)_2$ or an 8AF•FAD complex based on its wavelength. However, the former could only be produced by dimers of ETF and therefore would yield one CT complex per two ETFs, whereas an 8AF•FAD complex

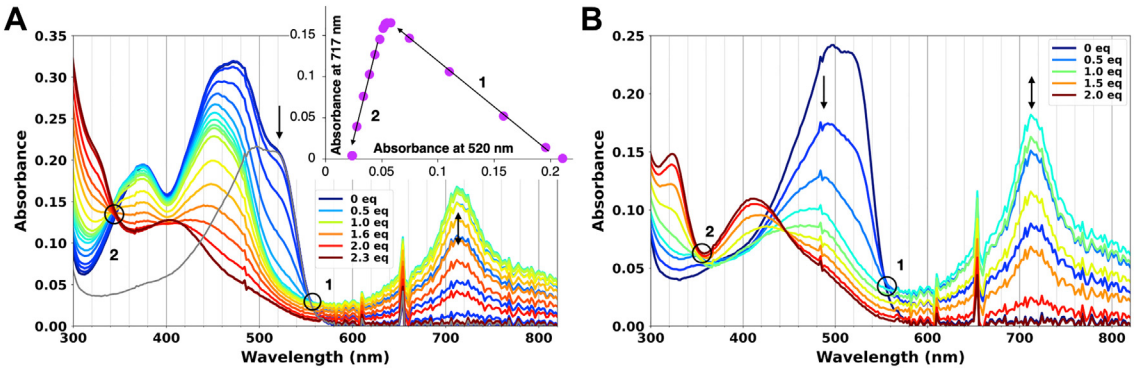

Figure 8. Comparisons of reductive titrations of 8AF in a 1:1 mixture with FAD *versus* alone. *A*, spectra collected in the course of stepwise reduction of a mixture of 15 μM each 8AF and FAD with Ti citrate as the reductant. The spectrum of precipitated and redissolved 8AF is shown in *gray* for comparison. In each case, the total flavin concentration was approximately 30 μM. The legend provides number of reducing equivalents present at selected points in the titration. An isosbestic characterizing the first phase is *circled* and numbered '1', whereas an isosbestic of the second phase is *circled* and numbered '2'. The inset plot of A_{717} *versus* A_{520} shows the sequential occurrence of the two phases, which are numbered in the same way. In phase 1, A_{717} grows with reduction of the 8AF whose OX state absorbs at 520 nm. In phase 2, A_{717} drops but in this case, the spectrum of FAD-OX is converted to that of FAD-HQ. The first point is on the *right*. The corresponding titration of 8AF alone is in panel *B*. Two phases are again clearly distinguished by A_{717} growth in the first *versus* shrinkage in the second.

could be formed by the ET and the Bf sites of a single ETF if a conformational change is invoked or within a dimer of ETFs that brings the ET site of one into contact with the Bf site of another, and *vice-versa*, to yield two CT complexes per two ETFs. Based on the relative strength of the 726 nm band observed in *Rpa*ETF (Fig. 6*A*) compared to its strength in a mixture of free FAD and 8AF (Fig. 8*A*), the protein greatly increases the favorability of complex formation, making a stoichiometry of one CT per ETF unit more probable and arguing for CT complexes involving an ET site with a Bf site. We previously invoked a conformational change to permit van der Waals contact between the two flavins within one ETF but now also consider that this could be accomplished by a dimer of two ETFs, based on our observation that flavin modification is accelerated at higher protein concentrations and the known tendency of ETF to form protein-protein associations (13, 20–22).

Significance for published E°s

Our current attribution of the 726 nm band to a complex containing a modified flavin reveals that some of our earlier work at high pH also included modified flavin, by accident (67). This could explain why our early work on WT *Rpa*ETF prepared at pH 9 yielded E°'s of $E°'_{OX/ASQ}$ =−47, $E°'_{ASQ/AHQ}$ = −83, and $E°_{OX/AHQ}$ =−223 mV *versus* NHE (67), whereas they were −61, −122, and −243, respectively, for material maintained and characterized at pH 8 (38). Indeed, *Rpa*ETF maintained at pH 8 does not populate a 726 nm species (Fig. 9*B*), compared to *Rpa*ETF maintained at pH 9 (Fig. 9*A*). The E° differences are not enormous, but they are significant. In particular, the *E°s* of the ET flavin are more separated for samples lacking 8AF, providing better stabilization of the ASQ state and thus better enforcement of the 1e transfer activity required of the ET flavin for most efficient bifurcation. For *Rpa*ETF maintained at pH 9, the stability constant of the ASQ at the potential that maximizes its population, $K_{sq} = [ASQ]^2/[OX][HQ] = 4$, whereas for *Rpa*ETF maintained at pH 8, $K_{sq} = 11$. In particular, the $E°'_{ASQ/AHQ}$ is

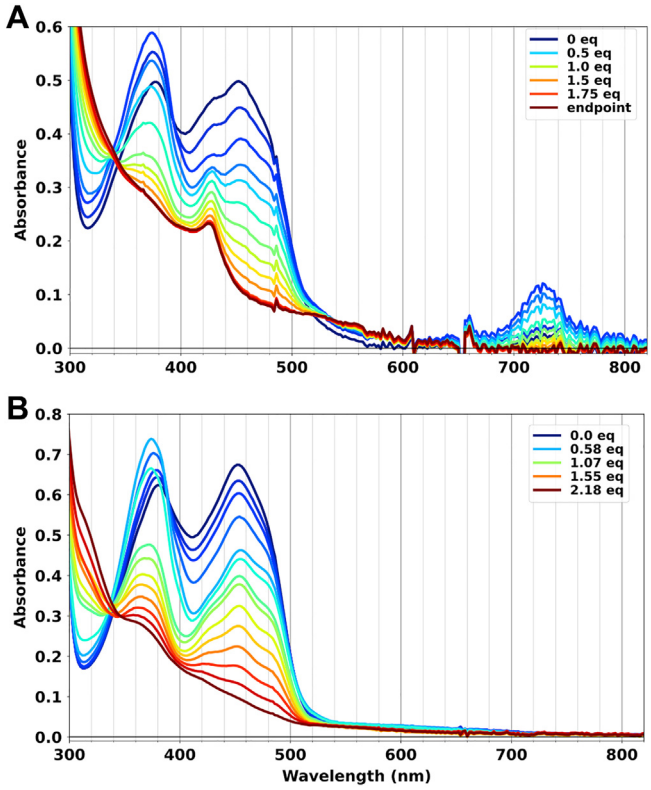

Figure 9. Effect of sample storage pH on the course and product of reduction. Reductive titrations of WT-*Rpa*ETF at *A*: pH 9 and *B*: pH 8. For a 30 μM sample of WT-*Rpa*ETF maintained and titrated at pH 8, negligible CT band at 726 nm was formed, whereas in a 24 μM sample of WT-*Rpa*ETF maintained and titrated at pH 9, considerable 726 nm band accumulated. Both samples were in 20 mM BTP buffer and only the pH differed. The sharp feature near 425 nm in panel A is most likely a reduced state of 8fF or 8AF (25). The amount of 726 nm band formed in panel *A* is consistent with this sample's modest 2 to 3 h tenure at pH 9, as needed for buffer transfer and concentration, in contrast to the much longer incubations used to monitor modification to its end-point, for Figures 4 and 6. The titration at pH 8 was performed using sodium dithionite (NaDT) whereas the titration performed at pH 9 employed Ti citrate, but prior work showed that the identity of the reductant does not alter formation of the 726 nm band (35, 67). Attainment of an endpoint was tested by waiting 15 to 30 min and then collecting an additional spectrum. Once spectra ceased to change, the titration was deemed complete, as shown in panel A.

considerably lower for authentic ET-FAD, consistent with the separate phases of reduction shown in Figure 9*B*. Since the E° values reported initially most likely reflected a significant population of 8AF or 8fF formed on the time scale of experiments conducted at pH 9, only the more recent values should be used (38).

Discussion

Our new results make sense of several perplexing spectral signatures (35) and shifted E°s (67). Crucially, they underscore the remarkable reactivity conferred by the ET site of ETF. ETFs are notorious for their formation of 8-OH and 6-OH flavins, which have been documented since 1974 (16, 68). The fact that *Mel*ETF was found to contain significant amounts of 8-OH flavin in its ET site, as isolated, demonstrates that breakage of the C-C bond attaching C8M to the xylene ring is facilitated (24). Sato *et al* isolated *Mel*ETF without modification, but the ET flavin was reconstituted to the protein rather than copurified, so their report is consistent with our finding that it is primarily the ET flavin that is modified (15). Additionally, their work was conducted in phosphate buffer at pH 6, thereby suppressing modification and accounting for the absence of 8fF formation. Moreover, the reaction is slow enough that it may have been avoided or not detected in other systems, which have not usually been maintained at elevated pHs. Thus, 8AF is unprecedented as an 'accidental' occurrence in ETFs, despite the numerous variants already reported for these proteins (16, 24–26, 68), so we infer that 8AF is not formed in abundance *in vivo*. Of wider significance, we find that amine buffers, especially at pHs above their pK_as, should not be assumed to be benign. On the contrary, we demonstrate that the ET site can enable amines to displace the C attached to the 8 position of the flavin. This opens exciting possibilities for producing modified flavins for other uses. Consequently, one would like to know what features of the ET site are responsible for this reactivity.

Production of modified flavin and possible significance of methide formation as a side-effect of ASQ stabilization

It is too early to establish the mechanism by which 8AF is formed in ETF, but our data offer some clues. Therefore, we present a model that seeks to associate our observations with a proposed sequence of events, to be tested by future work (Scheme S3). Based on our data and precedent (45, 47), we propose that (1) 8fF is an intermediate in formation of 8AF, (2) 8fF formation is promoted by methide tautomer stabilization by ET site residues, and (3) the site attracts OH^- as the O atom donor. Although 8fF did not accumulate as an intermediate at high ETF concentrations, its formation and consumption could be observed in more dilute reactions, consistent with mechanisms proposed for enzymatic 8AF formation (45, 47, 69). Conversion of 8fF to 8AF does not appear to require O_2, or tautomers enabled by the OX flavin π system, since it occurred anaerobically. However, it may involve radical-mediated bond migration and eventual recombination to yield 8AF-HQ (4). We propose that further conformational change and/or dimerization of two ETFs then yields the 726 nm CT species.

Our proposal that the ET site stabilizes a methide-like state of the ET flavin is based on literature mechanisms for 8fF formation, which call for delocalization of electron density from C8M to the flavin's N1-O2 locus as a result of HO^- attack on the C8M and/or deprotonation of the C8M to form a paraquinoid methide tautomer (Schemes S1 and S2 and (43, 45, 47, 70, 71)). Methyl groups do not normally ionize under physiological conditions, but the 8-methyl protons of flavin were found to exchange with water at pH 6.8 and 90 to 95 °C, indicating that a deprotonated state is accessible, if only *via* transient tautomerization (Schemes S1 and S2) (72, 73). Moreover, positive charge near N1-O2 is seen to favor 8fF formation (46), as well as covalent attachment of flavin to protein nucleophiles *via* the flavin C8M (71), supporting reaction *via* a methide intermediate (Scheme S2) (74, 75). Models of *Rpa*ETF indicate that a conserved His side chain donates a H-bond to the ET flavin O2 with a conserved Tyr side chain in turn donating a H-bond to the His (Fig. S8, bottom right). The same motif is seen in the *Mel*ETF found by Massey *et al.* to stabilize the benzoquinoid state of 8-mercaptoflavin (65). Thus, we expect that *Rpa*ETF's ET site can populate the proposed methide intermediate (Scheme S3).

We propose that population of methide tautomer may correlate with stabilization of the ASQ state by the ET site. A distinguishing functional feature of ETFs in general is their stabilization of the ASQ state of the ET flavin, which underpins its function as a 1e carrier (5, 38). We note that the ASQ state is only marginally stable for free flavin (28). However, the $E°'_{OX/ASQ}$ of *Rpa*ETF's ET flavin is −61 mV *versus* N.H.E. (38), compared to −313 mV for free flavin (28), indicating a 24 kJ/mol stabilization of ASQ relative to OX, in the ET site. Because the methide is also anionic, we propose that the very interactions that stabilize ASQ may also stabilize methide-like intermediates in 8fF formation. In support, stabilization of the benzoquinoid tautomer was found to correlate with stabilization of the ASQ (76). Indeed, the *Rpa*ETF variants that formed less 8AF (Fig. S3) also stabilized less ASQ (38). Thus, susceptibility to modification may constitute a general occupational hazard, for proteins that stabilize flavin ASQ.

The problem may be particularly acute for the ET flavin of ETF due to the surface exposure of the flavin dimethyl benzene ring in ETF's open conformation (Fig. S1). The ETFs that exist primarily in stable complexes with partner proteins may be less susceptible, as the bound partner protein may occlude the ET flavin from potential modifiers in solution. Other enzymes needing such reactivity or stabilizing anionic states of flavin may bury the flavin (77, 78), cover it with bound substrate (79), or passivate the flavin by committing an amino acid side chain to a covalent bond with the C8M (74). In contrast, it appears that biology exploits posttranslationally generated 8fF with its elevated ASQ stability to enhance catalytic activity in formate oxidase (43).

Besides residues near N1 and O2, a basic residue near C8M has been proposed to accelerate formation of 8fF, either by positioning OH^- to attack C8M (43) or by deprotonating the

C8M methyl (45). Doubayashi *et al.* and Robbins *et al.* have demonstrated that high pH and an Arg near C8M accelerate at least one of the steps in 8fF formation (43, 46). Our substitutions of Arg-273 demonstrate that in *Rpa*ETF as well, positive charge in this position is required for flavin modification (Fig. S3). Since the side chain or Arg-273 is adjacent to the C8M, Arg273 could recruit OH^- to that position from whence it could attack C8M, especially at the high pH that favors reaction of *Rpa*ETF. Thus, multiple factors may contribute, and their relative importance is likely to vary among flavin-binding sites. However, the above two motifs in *Rpa*ETF's ET site (Fig. S8) are consistent with *Rpa*ETF's formation of 8fF *via* a methide intermediate and attack by OH^-.

Since the flavin present at the start of the reactions was mostly unmodified and OX (blue curves in panels 4A and 4B) but became reduced beyond the ASQ state in anerobic reactions, it appears that the isoalloxazine ring system absorbs two of the four reducing equivalents lost in formation of 8fF (see Scheme S2). The simplest possibility is that sufficient residual O_2 is present in the early phases of sample degassing to accept two more reducing equivalents and thereby permit attack by a second OH^- and dehydration to yield reduced 8fF (Scheme S3). One molecule of O_2 per two ETFs would require ≈ 0.17 mM O_2, which is within the concentration dissolved in air-equilibrated buffer. Our MS data argue against presence of a hydroxyl on the C8M in the initial *Rpa*ETF; however, the possibility of cryptic disulfide linkages as oxidants also deserves investigation, in future work. Robbins *et al.* offer the interesting suggestion that reducing equivalents could be accepted by a protein residue that had formed a covalent link to the flavin (43), although initial formation of the adduct would have required oxidation by two equivalents (48) (Scheme S2). Our proposed nucleophilic attack by OH^- would be a variation on the same theme and would allow water to be the source of the O of 8fF. This contrasts with literature proposals that generally invoke O_2 as both the source of the O atom (47, 69) as well as the acceptor of reducing equivalents (43, 45), but our proposal is supported by Konjik *et al.*'s demonstrations using $H_2{}^{18}O$ that the added carbonyl O of 8fF can derive from water (47).

One reason that literature mechanisms for forming 8AF invoke so many oxidizing equivalents is that many assume departure of C8M as formate (45) or CO_2 (47, 69) which are highly oxidized, and the hydrogens displaced from the 8-methyl group in the course of its oxidation are also portrayed as being oxidized to H_2O. If we contemplate reduced biproducts instead, the requirement for an oxidant can be diminished. Moreover, if we recall the small radical population seen, as well as Konjik's determination that thiamine is required for RosB activity (47), in conjunction with established radical mechanisms supported by thiamine (80), we can entertain possibilities raised by bond migration and homolysis of the bond attaching C8M to the ring. The small amount of radical accumulated under our conditions could not account for the reducing equivalents involved, however, it could nevertheless be on-pathway, since it disappeared in conjunction with conversion to 8AF-HQ signaled by appearance of the 726 nm band. The fact that the reaction was faster at higher *Rpa*ETF concentrations also supports the possibility of a radical mechanism, which would conclude *via* recombination. Finally, a radical mechanism would be consistent with our MS data showing buffer-flavin adducts retaining only part of the parent buffer molecule. These observations imply that the nonflavin product could contain another fragment from the buffer. This could be united with a formyl fragment or even a less oxidized C8M. Fragmentation of alkyl amines such as our buffers was also seen when they were consumed as sacrificial reductants by photoexcited flavins (81), although we note that the relevance of photochemistry is limited, since the current reactions were always protected from light. Thus, resolution of such details must await definitive identification of the nonflavin product(s). In the meantime, our proposed sequence of events exploits well-known carbonyl chemistry. This predicts nonflavin products that depend on the identity of the buffer present and so will be readily testable.

We have shown that a modified flavin is responsible for the sharp CT band formed in *Rpa*ETF at pH 9 in BTP. Specifically, we found that the 726 nm signal is not due to flavin SQ and confirmed that it is best explained by a HQ•OX CT complex including a modified flavin in its HQ state. Indeed, the modified flavin sufficed to produce a sharp CT band near 717 nm, in the presence of BTP at pH 9. The modified flavin in question turned out to be an 8AF wherein the amino adduct was derived from the buffer present and indeed varied with buffer identity. The CT bands formed in different amine-based buffers were not distinguishable, in part due to their band widths. However, this is consistent with computations indicating that distinct spectral properties of 8AF derive mainly from the N atom's nonbonding lone pair conjugated into the π system and less on the particulars of the alkyl groups attached to the N (82). This enigmatic band can also be seen in figures from other research groups and ETFs from organisms other than *R. palustris*.

Finally, our time courses demonstrate that the 8AF is fully formed before the 726 nm band achieves full amplitude, consistent with our demonstration that 8AF is necessary, and sufficient in the presence of BTP. The CT complex observed in *Rpa*ETF is composed of an 8AF and an FAD rather than interaction between 8AFs in the ET sites of two ETFs, because the 726 nm CT band was maximal after the ET 8AF had been fully reduced to the HQ, rather than half-way through reduction of the ET flavin (35). We previously proposed that the 726 nm band reflects a complex between the two flavins of a single ETF, because it was not observed in the T94,97A variant lacking Bf flavin (35). We now interpret that result as a consequence of the instability of the variants lacking the Bf flavin (38), in conjunction with the slowness with which the required 8AF forms. Thus, a complex between ET flavin of one ETF and Bf flavin from another ETF is another possible explanation for the CT band at 726 nm and would be consistent with the concentration dependence of 8AF formation and growth of 726 nm band (Fig. S4). In the open conformation, the ET flavin is exposed on the surface of the ETF and the Bf flavin's xylene ring also protrudes from the

protein (13, 14, 19, 20). Thus, an interaction between two ETFs consistent with our concentration dependence could possibly explain the 726 nm band in terms of Bf-OX of one ETF making contact with 8AF-HQ in the ET site of another ETF (and *vice-versa*). However, we find this less likely based on the high yields of 726 nm band formed.

Contact between two flavins and implications for conformational change or protein associations

On mechanistic grounds, we remain intrigued by the original proposal that a conformational change allows the ET flavin to make contact with the Bf flavin in the same ETF (35). This is supported by the known ability of ETF's head domain to rotate and move the ET flavin relative to the Bf flavin (13, 14). Since no conformation has yet been observed experimentally that brings the two flavins of ETF close enough for direct electron transfer (19), the state in which this occurs must be short-lived and/or relatively unstable. However, our data on free flavins demonstrate that the 8AF forms a better-defined more stable CT complex with FAD than does FAD alone, allowing the possibility that an analogous complex in ETF incorporating 8AF is similarly more favorable than the naturally occurring conformation in which electron transfer actually occurs between two unmodified FADs. Thus, we speculate that the CT band we can now better explain, near 726 nm, might represent a mechanistically relevant conformational intermediate: a conformation in which electron transfer from the Bf to the ET flavin occurs *via* direct electron transfer within a CT complex. Such a mechanism would help to maximize the efficiency of bifurcation (35).

Concluding remarks

We have identified a new variant of FAD in which the C8M of FAD is replaced by an alkyl amine fragment of an amine-based buffer. The resulting 8AF appears to form from the 8fF documented by other authors in the ET site of ETF, specifically. The nature of the fragment added to the flavin depends on the identity of the buffer provided, but the adducts are 8AFs based on their optical spectra, NMR, and pH dependence, and they present considerable chemical and spectroscopic opportunities. Specifically, this 8AF explains the unusually well-defined CT band previously reported in half-reduced *Rpa*ETF in terms of an 8AF-HQ • FAD-OX CT complex, as it can form such a CT complex even in the absence of protein, when BTP is present. Formation of the CT band in Bf ETF demonstrates that two flavins can achieve van der Waals contact, implying either association of two ETFs or a conformational change that brings the ET flavin into contact with the Bf flavin within one ETF. Even a transient van der Waals complex between the two flavins would provide a high-efficiency mechanism for electron transfer between them. The fact that 8AF did not form from free FAD underscores the extent to which the ET site perturbs the reactivity of its bound flavin. Thus, the mechanisms by which 8fF and 8AF form provide new sources of insight into the tuning applied by the ET site that accomplishes the remarkable feat of stabilizing the ASQ state required for bifurcation. We propose that the interactions responsible also prime the bound flavin for oxidation to 8fF, for example, by stabilizing methide character.

Experimental procedures

Protein purification

WT-*Rpa*ETF was expressed in NiCo21(DE3) *Escherichia coli* cells bearing plasmids encoding *Rpa*EtfA with an N-terminal His_6 tag and *Rpa*EtfB with a C-terminal His_6 tag from the genes *fixB* and *fixA*, respectively (67). The strain also contained the plasmid pGro7 (Takara Bio) that encodes the chaperones groES/EL. Cells were grown in 1l of Terrific Broth supplemented with 20 mg/l riboflavin and 2 mM $MgSO_4$ along with carbenicillin (100 μg/ml), spectinomycin (100 μg/ml), and chloramphenicol (50 μg/ml) at 37 °C, shaking at 250 rpm, to an optical density at 600 nm of ∼1 to 2. After cooling the culture to 18 °C, groES/EL gene expression was induced with 1 mg/ml L-arabinose. After 30 min further growth, ETF gene expression was induced with 0.1 mM IPTG. Cultures were then grown for an additional 20 h at 18 °C. Cells were harvested by centrifugation at 4500 rpm, 4 °C for 30 min, and the pellet was stored at −80 °C after washing once in PBS (10 mM Na_2HPO_4, 1.8 mM KH_2PO_4, 137 mM NaCl, 2.7 mM KCl, pH 7.4).

Frozen cell pellet (∼30 g) was resuspended on ice in 60 ml of BugBuster (EMD Millipore) containing 1 mM 4-(2-aminoethyl)benzenesulfonyl fluoride hydrochloride (AEBSF, protease inhibitor), 1 mM FAD (Chem-Impex International), 2 μl of Benzonase Nuclease HC, and 2 μl of rLysozyme Solution (EMD Millipore) and further incubated at 4 °C for 2 h with stirring. After centrifugation at 15, 000 *g* for 30 min at 4 °C to remove debris, the supernatant was mixed with 1.5 ml of nickel-nitrilotriacetic acid resin (EMD Millipore) pre-equilibrated in buffer containing, 20 mM Tris, pH 7.8, 500 mM KCl. After stirring incubation of the cell lysate at 4 °C with resin for 30 min, the mixture was transferred to a column at 4 °C. After collecting the flow-through, the column was washed with 20 column volumes of 20 mM Tris, pH 7.8, 500 mM KCl containing 20 mM imidazole. Finally, the column was developed with two column volumes of 20 mM Tris, pH 7.8, 500 mM KCl containing 100 mM imidazole, and the eluate was collected in three fractions. After SDS-PAGE analysis of the fractions, those containing pure *Rpa*ETF were pooled and imidazole was removed by passage over a 10DG gel filtration column (Bio-Rad) equilibrated with 20 mM BTP, pH 9.0, 200 mM KCl, 10% (w/v) glycerol (working buffer). Because the affinity chromatography was always performed at lower pH, with transfer to pH 8 or 9 only occurring afterward, we describe samples as having been purified *into* pH 8 or pH 9, rather than saying that they were purified *at* one of those pHs. To fully populate all flavin-binding sites, the protein was incubated overnight in 1 mM FAD at 4 °C in darkness. Excess flavin was then removed by gel filtration on a 10DG column pre-equilibrated with working buffer (or the pH 8 equivalent) and concentrated to 400 to 800 μM in a 10 kDa cutoff

centricon, in a process that took 2 to 3 h. Material was used immediately thereafter.

The T94,97A ETF variant of *Rpa*ETF was overexpressed from genes encoding an N-terminally His tagged EtfA and a C-terminally His tagged EtfB incorporating the two mutations. Plasmid-bearing NiCo21 cells were grown in Terrific Broth medium supplemented with 20 mg/ml riboflavin, 20 mg/l adenosine 5-monophosphate, 2 mM $MgSO_4$, 100 μg/ml carbenicillin, and 100 μg/ml of spectinomycin. Cultures were grown at 37 °C, with shaking at 250 rpm until they reached an optical density at 600 nm of ∼1 and then cooled to 18 to 20 °C. Gene expression was induced with 0.1 mM IPTG and the cultures were then grown for 20 h at 18 to 20 °C. Cells were harvested by centrifugation at 11,900*g* at 4 °C for 10 min. Harvested cells (10 g/l culture) were washed with PBS and then lysed by resuspending in 80 ml of BugBuster (primary amine free, Millipore) supplemented with 1 mM AMP, 2 μl/80 ml benzonase nuclease (HC, 250 U/μl,), 2 μl/80 ml lysozyme (30 kU/μl), 1 mM TCEP (tris(2-carboxyethyl) phosphine), and 1 mM AEBSF protease inhibitor and incubated at 4 °C with stirring for 2 h. Insoluble material was removed by centrifugation at 15, 000*g* for 45 min at 4 °C.

Clarified cell lysate was mixed with 1.5 ml of Co-nitrilotriacetate resin (Thermo Fisher, Cat. No. 89966) that had been pre-equilibrated with 3 ml of equilibration buffer containing 20 mM Tris pH 7.4, 500 mM KCl, 10% w/v glycerol, and 1 mM TCEP. After a binding interval of 30 min with gentle stirring at 4 °C, protein-bound resin was loaded into a column (2.5 × 30 cm) and washed with 20× bed volumes of wash buffer containing 20 mM Tris pH 7.4, 500 mM KCl, 10% (w/v) glycerol, 1 mM TCEP, and 20 mM imidazole. Protein was eluted with two bed volumes of elution buffer containing 20 mM Tris pH 7.4, 500 mM KCl, 10% (w/v) glycerol, 1 mM TCEP, and 100 mM imidazole. The resulting pure ETF fractions were transferred to working buffer (or working buffer at pH 8, as indicated) by gel filtration on a pre-equilibrated DG10 column (Bio Rad) and then concentrated to 100 μM in a 10 kDa cutoff centricon, in a process that took 2 to 3 h generally, but see figure captions for special cases.

Flavin content of the Rpa*ETF*

The protein concentration (μg/ml) was determined using the Pierce 660 nm protein assay with bovine serum albumin as the standard (Cat. No. 23208, Thermo Fisher scientific). From this, the *Rpa*ETF concentration was calculated based on the molecular mass of 74, 545 Da (67). Purity was assessed *via* SDS-PAGE to be 90% or higher.

Cofactors were released from 350 μl of ∼30 μM *Rpa*ETF in working buffer, contained in a 1.5 ml microcentrifuge tube wrapped in aluminum foil to exclude light and prevent photochemical transformation of cofactors. *Rpa*ETF was denatured by heating at 100 °C for 10 min and then removed by centrifugation at 14,000*g* for 10 min after cooling the samples. Supernatant was transferred to a quartz cuvette and the optical spectrum was recorded on a HP 8453 spectrophotometer. Absorbance at 450 nm was used to determine the released FAD concentration (ε_{450} = 11.3 mM^{-1} cm^{-1} (17)).

Aerobic and anaerobic reactions

Samples were shielded from light and held at 4 °C for the duration of all reactions

Aerobic flavin modification was conducted using freshly purified *Rpa*ETF in the working buffer. Immediately upon purification, approximately 100 μM *Rpa*ETF in a microfuge tube was wrapped in aluminum foil and stored at 4 °C. An aliquot withdrawn at the start was named the 0 h sample. Reactions were sampled at intervals by removal of an aliquot. At each time point, ∼10 μl was diluted to 300 μl in working buffer. After collection of an optical spectrum, the ETF was heat-denatured to release the cofactors and protein was removed by centrifugation. UV/visible spectra of the supernatants were recorded immediately using a HP 8453 spectrophotometer, and mass spectrometric analysis was performed at Georgia State University's mass spectrometry facility. To assess dependence on concentration, aerobic modification was performed with 100, 224, and 350 μM WT *Rpa*ETF.

Anaerobic incubations were conducted in darkness using larger quantities of protein to permit sampling at more time points. Immediately following purification and concentration (in air), approximately 400 μM WT *Rpa*ETF was equilibrated with an N_2 atmosphere for 15 min in 50 μl aliquots at room-temperature in the antechamber of a glove box (Belle Technology). The concentrated protein was then brought into the anaerobic chamber and placed at 4 °C in darkness. At the time of transfer into the anaerobic chamber, the '0 h' sample (≈10 μl) was removed and diluted into degassed working buffer for collection of an optical spectrum (HP 8452A spectrophotometer, Agilent technologies, refurbished by OLIS and equipped with a Quantum Northwest temperature controller, housed in the anaerobic chamber). Additional samples were withdrawn from the reaction and immediately characterized *via* their optical spectra, over several days. Immediately after collection of the spectrum, each sample was removed from the anaerobic chamber and cofactors were released and characterized, as detailed above. Sample volumes and dilution factors were recorded to permit correction for dilution in the spectra and flavin quantifications. In some cases, aliquots were also characterized by reductive titration or mass spectrometry at Georgia State University's facility.

Reductive titrations

Reductive titrations were performed in an inert atmosphere, monitored using a HP 8452A spectrophotometer (Agilent technologies) refurbished by OLIS and equipped with a Quantum Northwest temperature controller, inside a glove box (Belle Technology), using a 1 cm path length self-masking quartz cuvette (Cat. No.18-Q-10-GL14-C, Starna Cells) at room temperature. 8AF was separated from total released flavin by precipitation (48 h at 4 °C in darkness) and then resuspended in water or phosphate buffer (see details in figure

captions). Solutions of 8AF alone or in combination with FAD were reduced stepwise in water (pH 6.8) or 20 mM BTP buffer at pH 9, using Ti(III) citrate (ε_{340} = 0.74 mM^{-1} cm^{-1} (83)).

Displacement of the ET flavin using ADP

Freshly purified WT *Rpa*ETF (700 μM) in BTP buffer at pH 9 was stored in the anaerobic chamber at 4 °C for 4 to 5 days to accumulate the 726 nm signal. About 25 μl of this material with pre-accumulated 726 nm signal was diluted with the degassed working buffer to 350 μl, yielding a final protein concentration of 50 μM. The optical spectrum was collected under inert atmosphere. Then, 200 mM ADP was added, and optical spectra were collected every 30 min for 8 to 10 h.

EPR

Freshly purified *Rpa*ETF was degassed and taken into the anaerobic chamber. For the EPR analysis, around 25 μl of sample was collected in a capillary tube at the given time intervals. Both ends of the capillary tube were sealed using critoseal to maintain anaerobicity while the EPR signal was being collected. The flavodoxin neutral SQ was stable in these sealed capillaries for more than 2 h. For data collection, each capillary tube was placed in an EPR quartz tube which was in turn positioned in the center of the EPR resonator. Electron paramagnetic resonance experiments were performed on 370 μM *Rpa*ETF in working buffer using an EMX-plus X-band EPR spectrometer model (Bruker) with 9.87 GHz microwave frequency. A microwave power of 1.262 mW was used, based on its being found to be nonsaturating for both controls, Fremy's salt ($K_2(SO_3)_2NO$ (84)) and flavodoxin, and the radicals in *Rpa*ETF. Modulation amplitude was 4.0 G at a modulation frequency of 100 kHz. Samples were run at 295 K in 50 μl capillaries and 32 scans with a conversion time of 16.00 ms, a time constant of 5.12 ms, and a sweep time of 33 s. The magnetic field was scanned from 3420 to 3620 G. The field modulation amplitude and phase of the signal channel were calibrated with solid DPPH (α,α'-diphenyl-ß-picryl hydrazyl). EPR signal strengths were converted to spin concentrations responsible based on the double integral of each signal, compared to standard curves generated using flavodoxin neutral SQ and Fremy's salt, which agreed with one-another. The uncertainty associated with EPR signal integration is estimated to be ≈20% of each reported value (not 20% of a spin).

^{1}H-NMR spectroscopy

WT-*Rpa*ETF was allowed to react in pH 9 BTP buffer in darkness and inert atmosphere for 4 to 5 days, at which point it had turned dark green due to formation of the 726 nm species, demonstrating accumulation of 8AF. The material was then removed from the anaerobic chamber, heat denatured, and centrifuged to remove the colorless protein pellet. The dark orange supernatant containing both flavins was stored in the refrigerator at 4 °C for 2 to 3 days in darkness during which time red flakes precipitated leaving a yellow liquor. The latter was decanted to leave precipitated red flavin. The red precipitate was resuspended in D_2O. Thus, the sample contained both red flavin and residues of BTP buffer plus KCl and glycerol. An authentic FAD sample was generated by dissolving FAD (from Chem-Impex International) in D_2O. For the red flavin, the signal of residual HOD was suppressed using weak presaturation as implemented in Bruker's noesypr1d sequence. Chemical shift was referenced *versus* residual HOD at 4.7 ppm.

Mass spectrometry

Samples of 8AF were prepared from the red material that precipitated out of cold 20 mM BTP, by redissolving it in HPLC grade water. To monitor the 8fFAD, protein was transferred quickly into water *via* gel filtration and concentrated by ultrafiltration before being denatured to isolate the 8fFAD. Isolated flavins were shipped to Georgia State University along with purchased FAD dissolved in water, as a control. ESI-MS in negative ion mode (MS-ESI (-)) was carried out on a Waters Q-TOF micro-mass spectrometer, with the samples being infused directly at a 5 μl/min flow rate. The ESI tuning settings were capillary voltage at 3000, sample cone voltage at 40, extraction voltage at 1, desolvation temperature at 100 °C, and source temperature at 70 °C.

Stability constant of ASQ

The stability constant of the ASQ at the potential that maximizes its population, K_{sq} was calculated from the values of $E^\circ_{OX/ASQ}$ and $E^\circ_{ASQ/HQ}$ as per Mayhew noting that Mayhew denotes $E^\circ_{OX/ASQ}$ as E°_2 and $E^\circ_{ASQ/HQ}$ as E°_1 (28).

$$K_{sq} = \frac{[ASQ]^2}{[OX][HQ]} \text{ and}$$
$$K_{sq} = 10\frac{2.303F}{RT}\left(E^o_{\ OX/HQ} - E^o_{\ SQ/HQ}\right) \quad (1)$$

(85)

Structural model of RpaETF

*Rpa*ETF's sequence was modeled on the crystal structure of *Acidaminococcus fermentans* ETF 4KPU.pdb with which it shares 40% identity (19), and the resulting structure was validated *via* computation and spectroscopy (23).

Data availability

Data are all provided, either contained in the article or in the supporting information.

Supporting information—This article contains supporting information (13, 19, 25, 42, 43, 45, 47, 53, 66, 69, 71, 76–78, 86–93).

Acknowledgments—We express appreciation to supportive colleagues and proactive critics who made it possible for us to correct a critical knowledge gap. We thank S. Wang and A. Iyer (Georgia State University), D. Heidary, E. C. Glazer, N. Kothalawala, and D. Kim (University of Kentucky) for access to instrumentation, K.

Ranguelova (Bruker Biospin) for guidance in EPR, H. D. Duan for careful foundational work, and R. Murthy.

Author contributions—N. M.-R. and A.-F. M. conceptualization; N. M.-R. and A.-F. M. methodology; N. M.-R., C. v. G., R. S., and A.-F. M. validation; N. M.-R., C. v. G., and R. S. investigation; N. M.-R. and A.-F. M. writing–original draft; N. M.-R. and A.-F. M. writing–review and editing; N. M.-R. and A.-F. M. visualization; R. S. and A.-F. M. resources; A.-F. M. supervision; A.-F. M. funding acquisition.

Funding and additional information—N. M. R. and A.-F. M. acknowledge partial support from N.S.F. CHE 1808433 and CHE 2108134, and A.-F. M. additionally acknowledges partial support from D.O.E. DE-SC0021283 and the Einstein Foundation of Berlin for a visiting fellowship. C. V. G., and R. J. S. gratefully acknowledge partial support from the National Atmospheric and Space Administration's Exobiology program (80NSSC17K0033).

Conflict of interest—The authors declare that they have no conflicts of interest with the contents of this article.

Abbreviations—The abbreviations used are: 8fF, 8-formyl flavin; 8AF, 8-amino flavin; ASQ, anionic semiquinone; Bf, bifurcating; BTP, 1,3-bis[tris(hydroxymethyl)amino]propane; CT, charge-transfer; ESI-MS, electrospray ionization mass spectrometry; ET, electron transfer; ETF, electron transferring flavoprotein; HQ, hydroquinone; LF, lumiflavin; OX/ASQ, oxidized/anionic semiquinone; TCEP, tris(2-carboxyethyl) phosphine.

References

1. Crane, K. L., and Beinert, H. (1956) On the mechanism of dehydrogenation of fatty acyl derivatives of coenzyme A. II. The electron transferring flavoprotein. *J. Biol. Chem.* **218**, 717–731
2. Byron, C. M., Stankovich, M. T., Husain, M., and Davidson, V. L. (1989) Unusual redox properties of electron-transfer flavoprotein from *Methylophilus methylotrophus*. *Biochemistry* **28**, 8582–8587
3. Steenkamp, D. J., and Gallup, M. (1978) The natural flavoprotein electron acceptor of trimethylaminne dehydrogenase. *J. Biol. Chem.* **253**, 4086–4089
4. Watmough, N. J., and Frerman, F. E. (2010) The electron transfer flavoprotein: ubiquinone oxidoreductases. *Biochim. Biophys. Acta* **1797**, 1910–1916
5. Thorpe, C. (1991) Electron-transferring flavoproteins. In: Müller, F., ed. *Chemistry and Biochemistry of Flavoenzymes*, CRC press, Boca Raton FL: 471–486
6. Toogood, H. S., van Thiel, A., Basran, J., Sutcliffe, M. J., and Scrutton, N. S. (2004) Extensive domain motion and electron transfer in the human electron transferring flavoprotein·medium chain acyl-CoA dehydrogenase complex. *J. Biol. Chem.* **279**, 32904–32912
7. Roberts, D. L., Frerman, F. E., and Kim, J. J. (1996) Three-dimensional structure of human electron transfer flavoprotein to 2.1-A resolution. *Proc. Natl. Acad. Sci. U. S. A.* **93**, 14355–14360
8. Leys, D., Basran, J., Talfournier, F., Sutcliffe, M. J., and Scrutton, N. S. (2003) Extensive conformational sampling in a ternary electron transfer complex. *Nat. Struct. Biol.* **10**, 219–225
9. Roberts, D. L., Salazar, D., Fulmer, J. P., Frerman, F. E., and Kim, J. J. (1999) Crystal structure of paracoccus denitrificans electron transfer flavoprotein: structural and electrostatic analysis of a conserved flavin binding domain. *Biochemistry* **38**, 1977–1989
10. Sato, K., Nishina, Y., and Shiga, K. (1993) Electron-transferring flavoprotein has an AMP-binding site in addition to the FAD-binding site. *J. Biochem.* **114**, 215–222
11. DuPlessis, E. R., Rohlfs, R. J., Hille, R., and Thorpe, C. (1994) Electron-transferring flavoproteins from pig and the methylotrophic bacterium W3A1 contains AMP as well as FAD. *Biochem. Mol. Biol. Int.* **32**, 195–199
12. Toogood, H. S., van Thiel, A., Scrutton, N. S., and Leys, D. (2005) Stabilization of non-productive conformations underpins rapid electron transfer to electron transferring flavoprotein. *J. Biol. Chem.* **280**, 30361–30366
13. Demmer, J. K., Chowdhury, N. P., Selmer, T., Ermler, U., and Buckel, W. (2017) The semiquinone swing in the bifurcating electron transferring flavoprotein/butyryl-coA dehydrogenase complex from *Clostridium difficile*. *Nat. Commun.* **8**, 1577
14. Toogood, H. S., Leys, D., and Scrutton, N. S. (2007) Dynamics driving function: new insights from electron transferring flavoproteins and partner complexes. *FEBS J.* **274**, 5481–5504
15. Sato, K., Nishina, Y., and Shiga, K. (2003) Purification of electron-transferring flavoprotein from *Megasphaera elsdenii* and binding of additional FAD with an unusual absorption spectrum. *J. Biochem.* **134**, 719–729
16. Whitfield, C. D., and Mayhew, S. G. (1974) Purification and properties of electron-transferring flavoprotein from *Peptostreptococcus elsdenii*. *J. Biol. Chem.* **249**, 2801–2810
17. Sato, K., Nishina, Y., and Shiga, K. (2013) Interaction between NADH and electron-transferring flavoprotein from *Megasphaera elsdenii*. *J. Biochem.* **153**, 565–572
18. Chowdhury, N. P., Kahnt, J., and Buckel, W. (2015) Reduction of ferredoxin or oxygen by flavin-based electron bifurcation in Megasphaera Elsdenii. *FEBS J.* **282**, 3149–3160
19. Chowdhury, N. P., Mowafy, A. M., Demmer, J. K., Upadhyay, V., Koelzer, S., Jayamani, E., *et al.* (2014) Studies on the mechanism of electron bifurcation catalyzed by electron transferring flavoprotein (Etf) and butyryl-CoA dehydrogenase (Bcd) of *Acidaminococcus fermentans*. *J. Biol. Chem.* **289**, 5145–5157
20. Demmer, J. K., Bertsch, J., Oppinger, C., Wohlers, H., Kayastha, K., Demmer, U., *et al.* (2018) Molecular basis of the flavin-based electron-bifurcating caffeyl-CoA reductase reaction. *FEBS Lett.* **592**, 332–342
21. Kayastha, K., Katsyv, A., Himmrich, C., Welsch, S., Schuller, J. M., Ermler, U., *et al.* (2022) Structure-based electron-confurcation mechanism of the Ldh-EtfAB complex. *eLife* **11**, e77095
22. Feng, X., Schut, G. J., Lipscomb, G., Li, H. Y., and Adams, M. W. W. (2021) Cryoelectron microscopy structure and mechanism of the membrane-associated electron-bifurcating flavoprotein Fix/EtfABCX. *Proc. Natl. Acad. Sci. U. S. A.* **118**, e2016978118
23. Mohamed-Raseek, N., Duan, H. D., Mroginski, M. A., and Miller, A. F. (2019) Spectroscopic, thermodynamic and computational evidence of the locations of the FADs in the nitrogen fixation-associated electron transfer flavoprotein. *Chem. Sci.* **10**, 7762–7772
24. O'Neill, H., Mayhew, S. G., and Butler, G. (1998) Cloning and analysis of the genes for a novel electron-transferring flavoprotein from *Megasphaera elsdenii*. *J. Biol. Chem.* **273**, 21015–21024
25. Augustin, P., Toplak, M., Fuchs, K., Gerstmann, E. C., Prassl, R., Winkler, A., *et al.* (2018) Oxidation of the FAD cofactor to the 8-formyl-derivative in human electron-transferring flavoprotein. *J. Biol. Chem.* **293**, 2829–2840
26. Lehman, T. C., and Thorpe, C. (1992) A new form of mammalian electron transfer flavoprotein. *Arch. Biochem. Biophys.* **292**, 594–599
27. Herrmann, G., Jayamani, E., Mai, G., and Buckel, W. (2008) Energy conservation *via* electron-transferring flavoprotein in anaerobic bacteria. *J. Bacteriol.* **190**, 784–791
28. Mayhew, S. G. (1999) The effects of pH and semiquinone formation on the oxidation-reduction potentials of flavin mononucleotide: a reappraisal. *Eur. J. Biochem.* **265**, 698–702
29. Yang, K. Y., and Swenson, R. P. (2007) Modulation of the redox properties of the flavin cofactor through hydrogen-bonding interactions with the N(5) atom: role of alpha Ser254 in the electron-transfer flavoprotein from the methylotrophic bacterium W3A1. *Biochem* **46**, 2289–2297
30. Griffin, K. J., Dwyer, T. M., Manning, M. C., Meyer, J. D., Carpenter, J. F., and Frerman, F. E. (1997) alphaT244M mutation affects the redox,

kinetic, and *in vitro* folding properties of *Paracoccus denitrificans* electron transfer flavoprotein. *Biochemistry* **36**, 4194–4202
31. Schut, G. J., Mohamed-Raseek, N. R., Tokmina-Lukaszewska, M., Mulder, D. E., Nguyen, D. M. N., Lipscomb, G. L., *et al.* (2019) The catalytic mechanism of electron bifurcating electron transfer flavoproteins (ETFs) involves an intermediary complex with NAD+. *J. Biol. Chem.* **294**, 3271–3283
32. Pechter, K. B., Gallagher, L., Pyles, H., Manoil, C. S., and Harwood, C. S. (2015) Essential genome of the metabolically versatile alphaproteobacterium Rhodopseudomonas Palustris. *J. Bacteriol.* **198**, 867–876
33. Garcia Costas, A. M., Poudel, S., Miller, A.-F., Schut, G. J., Ledbetter, R. N., Fixen, K., *et al.* (2017) Defining electron bifurcation in the electron transferring flavoprotein family. *J. Bacteriol.* **199**, e00440-17
34. Su, D., Yuan, H., and Gadda, G. (2017) A reversible, charge-induced intramolecular C4a-S-cysteinyl-flavin in choline oxidase variant S101C. *Biochemistry* **56**, 6677–6690
35. Duan, H. D., Mohamed-Raseek, N., and Miller, A. F. (2020) Spectroscopic evidence for direct flavin-flavin contact in a bifurcating electron transfer flavoprotein. *J. Biol. Chem.* **295**, 12618–12634
36. Mewies, M., Basran, J., Packman, L. C., Hille, R., and Scrutton, N. S. (1997) Involvement of a flavin iminoquinone methide in the formation of 6-hydroxyflavin mononucleotide in trimethylamine dehydrogenase: a rationale for the existence of 8R-methyl and C6-linked covalent flavoproteins. *Biochem* **36**, 7162–7168
37. Walsh, C. (1980) Flavin coenzymes: at the crossroads of biological redox Chemistry. *Acc. Chem. Res.* **13**, 148–155
38. Mohamed-Raseek, N., and Miller, A. F. (2022) Contrasting roles for two conserved arginines: stabilizing flavin semiquinone or quaternary structure, in bifurcating electron transfer flavoproteins. *J. Biol. Chem.* **298**, 101733. **in press**
39. Dwyer, T. M., Zhang, L., Muller, M., Marrugo, F., and Frerman, F. E. (1999) The functions of the flavin contact residuesαArg249 and βTyr16, in human electron transfer flavoprotein. *Biochim. Biophys. Acta* **1433**, 139–152
40. Burgess, S. G., Messiha, H. L., Katona, G., Rigby, S. E. J., Leys, D., and Scrutton, N. S. (2008) Probing the dynamic interface between trimethylamine dehydrogenase (TMADH) and electron transferring flavoprotein (ETF) in the TMADH-2ETF complex: role of the Arg-α237 (ETF) and Tyr-442 (TMADH) residue pair. *Biochemistry* **47**, 5168–5181
41. Talfournier, F., Munro, A. W., Basran, J., Sutcliffe, M. J., Daff, S., Chapman, S. K., *et al.* (2001) Alpha Arg-237 in *Methylophilus methylotrophus* (sp. W3A1) electron-transferring flavoprotein affords approximately 200-millivolt stabilization of the FAD anionic semiquinone and a kinetic block on full reduction to the dihydroquinone. *J. Biol. Chem.* **276**, 20190–20196
42. Mohamed-Raseek, N. (2021) *Flavin Modification and Redox Tuning in The Bifurcating Electron Transfer Flavoprotein From Rhodopseudomonas Palustris: Two Arginines With Different Roles*, Ph. D., University of Kentucky, Lexington, KY
43. Robbins, J. M., Souffrant, M. G., Hamelberg, D., Gadda, G., and Bommarius, A. S. (2017) Enzyme-mediated conversion of flavin adenine dinucleotide (FAD) to 8-formyl FAD in formate oxidase results in a modified cofactor with enhanced catalytic properties. *Biochemistry* **56**, 3800–3807
44. Ghisla, S., and Mayhew, S. G. (1976) Identification and properties of 8-hydroxyflavin-adenine dinucleotide in electron transfer flavoprotein from *Peptostreptococcus elsdenii*. *Eur. J. Biochem.* **63**, 373–390
45. Jhulki, I., Chanani, P. K., Abdelwahed, S. H., and Begley, T. P. (2016) A remarkable oxidative cascade that replaces the riboflavin C8 methyl with an amino group during roseoflavin biosynthesis. *J. Am. Chem. Soc.* **138**, 8324–8327
46. Doubayashi, D., Oki, M., Mikami, B., and Uchida, H. (2019) The microenvironment surrounding FAD mediates its ocnversion to 8-formyl-FAD in Aspergillus oryzae RIB40 formate oxidase. *J. Biochem.* **166**, 67–75
47. Konjik, V., Brünle, S., Demmer, U., Vanselow, A., Sandhoff, R., Ermler, U., *et al.* (2017) The crystal structure of RosB: insights into the reaction mechanism of the first member of a family of flavodoxin-like enzymes. *Angew. Chem. Int. Ed.* **56**, 1146–1151
48. Jin, J., Mazon, H., van den Heuvel, R. H. H., Heck, A. J., Janssen, D. B., and Fraaije, M. W. (2008) Covalent flavinylation of vanillyl-alcohol oxidase is an autocatalytic process. *FEBS J.* **275**, 5191–5200
49. Song, p.-S., Walker, E. B., Vierstra, R. D., and Poff, K. L. (1980) Roseoflavin as a blue light receptor analog: spectroscopic characterization. *Photochem. Photobiol.* **32**, 393–398
50. Ghisla, S., Massey, V., and Mayhew, S. G. (1976) Studies on the active centers of flavoproteins: binding of 8-hydroxy-FAD and 8-hydroxy-FMN to apoproteins. In: Singer, T. P., ed. *Flavins and Flavoproteins*, Elsevier, Amsterdam: 334–340
51. Ghisla, S., and Mayhew, S. G. (1973) Identification and structure of a novel flavin prosthetic group associated with reduced nicotinamide adenine dinucleotide dehydrogenase from *Peptostreptococcus elsdenii*. *J. Biol. Chem.* **248**, 6568–6570
52. Moore, E. G., Ghisla, S., and Massey, V. (1979) Properties of flavins where the 8-methyl group is replaced by mercapto- residues. *J. Biol. Chem.* **254**, 8173–8178
53. Wang, Y., Sun, M., Qiao, J., Ouyang, J., and Na, N. (2018) FAD roles in glucose catalytic oxidation studied by multiphase flow of extractive electrospray ionization (MF-EESI) mass spectrometry. *Chem. Sci.* **9**, 594–599
54. Stewart, R. C., and Massey, V. (1985) Potentiometric studies of native and flavin-substituted old yellow enzyme. *J. Biol. Chem.* **260**, 13639–13647
55. Tyagi, A., Zirak, P., Penzkofer, A., Mathes, T., Hegemann, P., Mack, M., *et al.* (2009) Absroption and emission spectroscopic characterization of 8-amino-riboflavin. *Chem. Phys.* **364**, 19–30
56. Mayhew, S. G., and Ludwig, M. L. (1975) Flavodoxins and electron transferring flavoproteins. In: Boyer, P., ed. *The Enzymes*, Academic Press, NY: 57–118
57. Maeda-Yorita, K., Aki, K., Sagai, H., Misaki, H., and Massey, V. (1995) L-lactate oxidase and L-lactate monooxygenase: mechanistic variations on a common structural theme. *Biochimie* **77**, 631–642
58. Robbins, J. M., Geng, J., Barry, B. A., Gadda, G., and Bommarius, A. S. (2018) Photoirradiation generates an ultrastable 8-formyl FAD semiquinone radical with unusual properties in formate oxidase. *Biochemistry* **57**, 5818–5826
59. Barquera, B., Ramirez-Silva, L., Morgan, J. E., and Nilges, M. J. (2006) A new flavin radical signal in the Na+-pumping NADH"quinone oxidoreductase from *Vibrio cholerae*. *J. Biol. Chem.* **281**, 36482–36491
60. Edmondson, D. (1985) Electron spin resonance studies on flavoenzymes. *Biochem. Soc. Trans.* **13**, 593–600
61. Edmondson, D., Ackrell, B. A. C., and Kearney, E. B. (1981) Identification of neutral and anioni 3α-substituted flavin semiquinones in flavoproteins by electron spin resonance spectroscopy. *Arch. Biochem. Biophys.* **208**, 69–74
62. Gibson, Q. H., Massey, V., and Atherton, N. M. (1962) The nature of compounds present in mixtures of oxidized and reduced flavin mononucleotides. *Biochem. J.* **85**, 369–383
63. Beinert, H. (1956) Spectral characteristics of flavins at the semiquinoid oxidation level. *J. Am. Chem. Soc.* **78**, 5323–5328
64. Hopkins, N., and Stanley, R. J. (2003) Measurement of the electronic properties of the flavoprotein old yellow enzyme (OYE) and the OYE:p-Cl phenol charge-transfer complex using Stark spectroscopy. *Biochem* **42**, 991–999
65. Massey, V., Ghisla, S., and Moore, E. G. (1979) 8-mercaptoflavins as active-site probes of flavoenzymes. *J. Biol. Chem.* **254**, 9640–9650
66. Abramovitz, A. S., and Massey, V. (1976) Interaction of phenols with old yellow enzyme. *J. Biol. Chem.* **251**, 5327–5336
67. Duan, H. D., Lubner, C. E., Tokmina-Lukaszewska, M., Gauss, G. H., Bothner, B., King, P. W., *et al.* (2018) Distinct flavin properties underlie flavin-based electron bifurcation within a novel electron-transferring flavoprotein FixAB from *Rhodopseudomonas palustris*. *J. Biol. Chem.* **293**, 4688–4701
68. Mayhew, S. G., Whitfield, C. D., Ghisla, S., and M, S.-J. (1974) Identification and properties of new flavins in electron-transferring flavoprotein

from *Peptostreptococcus elsdenii* and pig-liver glycolate oxidase. *Eur. J. Biochem.* **44**, 579–591
69. Kapoor, I., and Nair, S. K. (2018) Structure-guided analyses of a key enzyme involved in the biosynthesis of an antivitamin. *Biochemistry* **57**, 5282–5288
70. Yorita, K., Matsuoka, T., Masaki, H., and Massey, V. (2000) Interaction of two arginine residues in lactate oxidase with the ezyme flavin: conversion of FMN to 8-formyl-FMN. *Proc. Natl. Acad. Sci. U. S. A.* **97**, 13039–13044
71. Heuts, D. P. H. M., Scrutton, N. S., McIntire, W. S., and Fraaije, M. W. (2009) What's in a covalent bond? On the role and formation of covalently bound flavin cofactors. *FEBS J.* **276**, 3405–3427
72. Bullock, F. J., and Jardetzky, O. (1965) An experimental demonstration of the nuclear magnetic resonance assignments in the 6,7-dimethylisoalloxazine nucleus. *J. Org. Chem.* **30**, 2056–2057
73. Hemmerich, P., Prijs, B., and Erlenmeyer, H. (1959) Studien in der lumiflavin-reihe V. Spezifische reaktivität 8-ständiger substituenten am isoalloxazin-kern. Flavin-dimere. *Helv. Chim. Acta* **27**, 2164–2177
74. Mewies, M., McIntire, W. S., and Scrutton, N. S. (1998) Covalent attachment of flavin adenine dinucleotide (FAD) and flavin mononucleotide (FMN) to enzymes: the current state of affairs. *Prot. Sci.* **7**
75. Brandsch, R., and Bichler, V. (1991) Autoflavination of apo6-hydroxy-D-nicotine oxidase. *J. Biol. Chem.* **266**, 19056–19062
76. Massey, V., and Hemmerich, P. (1980) Active site probes of flavoproteins. *Biochem. Soc. Trans.* **8**, 246–257
77. Mattevi, A., Vanoni, M. A., Todone, F., Rizzi, M., Teplyakov, A., Coda, A., *et al.* (1996) Crystal structure of D-amino acid oxidase: a case of active site mirror-image convergent evolution with flavocytochrome B2. *Proc. Natl. Acad. Sci. U. S. A.* **93**, 7496–7501
78. Xia, Z. X., and Mathews, F. S. (1990) Molecular structure of flavocytochrome b2 at 2.4 A resolution. *J. Mol. Biol.* **212**, 837–863
79. Choong, Y. S., and Massey, V. (1980) Stabilization of lactate oxidase flavin anion radical by complex formation. *J. Biol. Chem.* **255**, 8672–8677
80. Ragsdale, S. W. (2003) Pyruvate ferredoxin oxidoreductase and its radical intermediate. *Chem. Rev.* **103**, 2333–2346
81. Frisell, W. R., Chung, C. W., and Mackenzie, C. G. (1959) Catalysis of oxidation of nitrogen compounds by flavin coenzymes in the presence of light. *J. Biol. Chem.* **234**, 1297–1302
82. Kar, R. K., Chasen, S., Mroginski, M. A., and Miller, A. F. (2021) Tuning the quantum chemical properties of flavins *via* modification at C8. *J. Phys. Chem. B* **125**, 12654–12669
83. Seefeldt, L. C., and Ensign, S. A. (1994) A continuous, spectrophotometric activity assay for nitrogenase using the reductant titanium(III) citrate. *Anal. Biochem.* **221**, 379–386
84. Babcock, G. T., Ghanotakis, D. F., Ke, B., and Diner, B. A. (1983) Electron donation to photosystem II in reaction center preparations. *Biochim. Biophys. Acta* **723**, 276–286
85. Miller, A. F., Duan, H. D., Varner, T. A., and Mohamed-Raseek, N. (2019) Reduction midpoint potentials of bifurcating electron transfer flavoproteins. *Met. Enzymol.* **620**, 365–398
86. Smith, S. B., Brüstlein, M., and Bruice, T. C. (1974) Electrophilicity of the 8 position of the isoalloxazine (flavine) ring system. Comment on the mechanism of oxidation of dihydroisoalloxazine. *J. Am. Chem. Soc.* **96**, 3696–3697
87. Meng, E. C., Pettersen, E. F., Couch, G. S., Huang, C. C., and Ferrin, T. E. (2006) Tools for integrated sequence-structure analysis with UCSF Chimera. *BMC Bioinformatics* **7**, 339
88. Umena, Y., Yorita, K., Matsuoka, T., Kita, A., Fukui, K., and Morimoto, Y. (2006) The crystal structure of L-lactate oxidase from Aerococcus viridans at 2.1 Å resolution reveals the mechanism of strict substrate recognition. *Biochem. Biophys. Res. Commun.* **350**, 249–256
89. Iverson, T. M., Luna-Chavez, C., Croal, L. R., Cecchini, G., and Rees, D. C. (2002) Crystallographic studies of the Escherichia coli quinol-fumarate reductase with inhibitors bound to the quinol-binding site. *J. Biol. Chem.* **277**, 16124–16130
90. Doubayashi, D., Ootake, T., Maeda, Y., Oki, M., Tokunaga, Y., Sakurai, A., *et al.* (2011) Formate oxidase, an enzyme of the glucose- methanol-choline oxidoreductase family, has a His-Arg pair and 8-formyl-FAD at the catalytic site. *Biosci Biotechnol Biochem* **75**, 1662–1667
91. Arnold, K., Bordoli, L., Kopp, J., and Schwede, T. (2006) The SWISS-MODEL Workspace: A web-based environment for protein structure homology modelling. *Bioinformatics* **22**, 195–201
92. Waterhouse, A., Bertoni, M., Bienert, S., Studer, G., Tauriello, G., Gumienny, R., *et al.* (2014) SWISS-MODEL: homology modelling of protein structures and complexes. *Nucleic Acids Res* **46**, W296–W303
93. Pettersen, E. F., Goddard, T. D., Huang, C. C., Couch, G. S., Greenblatt, D. M., Meng, E. C., *et al.* (2004) UCSF Chimera - a visualization system for exploratory research and analysis. *J. Comput. Chem.* **25**, 1605–1612